Light flavour hadron production in the ALICE experiment at LHC

Angela Badalà
INFN Sezione di Catania
for the ALICE Collaboration

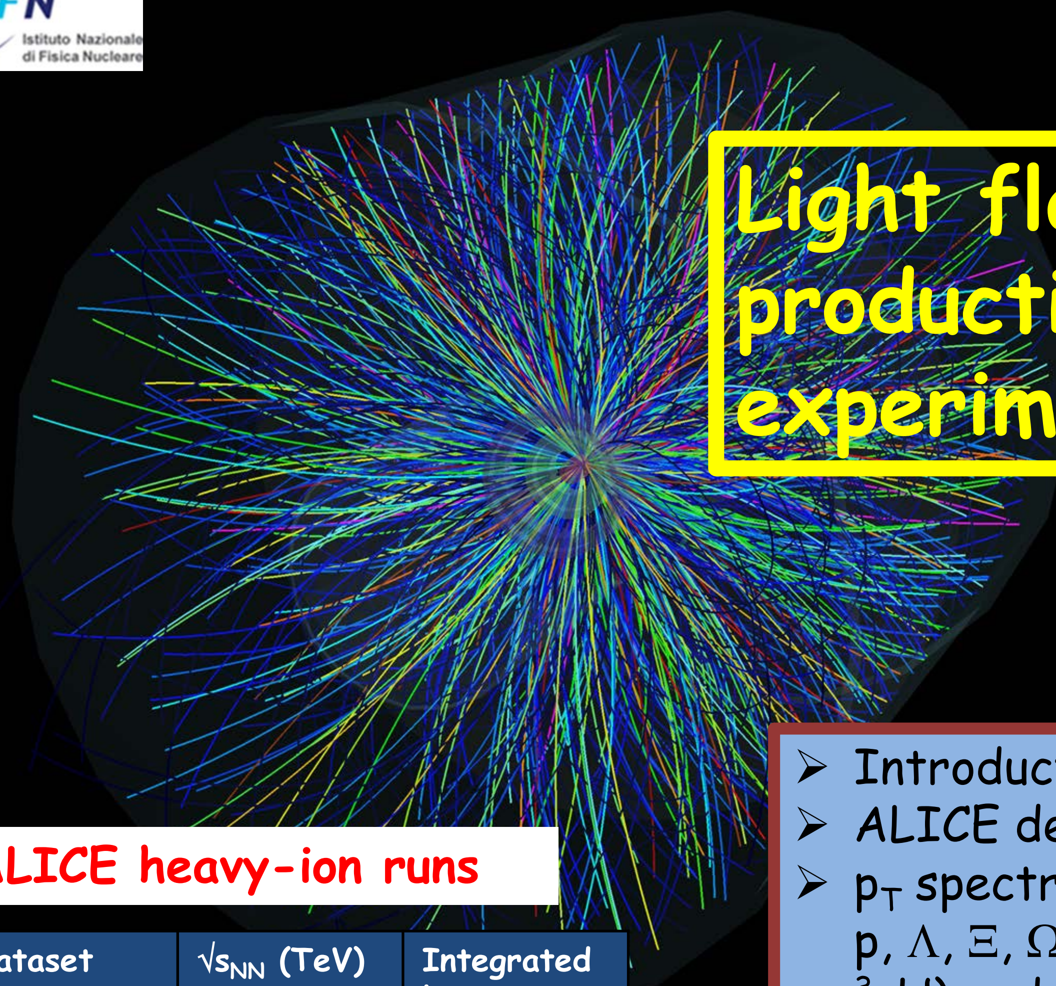

- Introduction
- ALICE detector
- p_T spectra of light flavour hadrons (π, K, p, Λ, Ξ, Ω, d, (anti-)nuclei (^{3}He, ^{4}He) and $^3_\Lambda$H) and comparison with hydrodynamical models in Pb-Pb and p-Pb
- Baryon-meson ratios (Pb-Pb, p-Pb)
- Ξ/π, Ω/π and d/p ratios (Pb-Pb, p-Pb)
- Thermal model results (Pb-Pb, p-Pb)
- Summary

ALICE heavy-ion runs

Dataset	$\sqrt{s_{NN}}$ (TeV)	Integrated luminosity
2010 Pb-Pb	2.76	~10 μb^{-1}
2011 Pb-Pb	2.76	~0.1nb^{-1}
2013 p-Pb	5.02	~0.1nb^{-1}

Our current picture

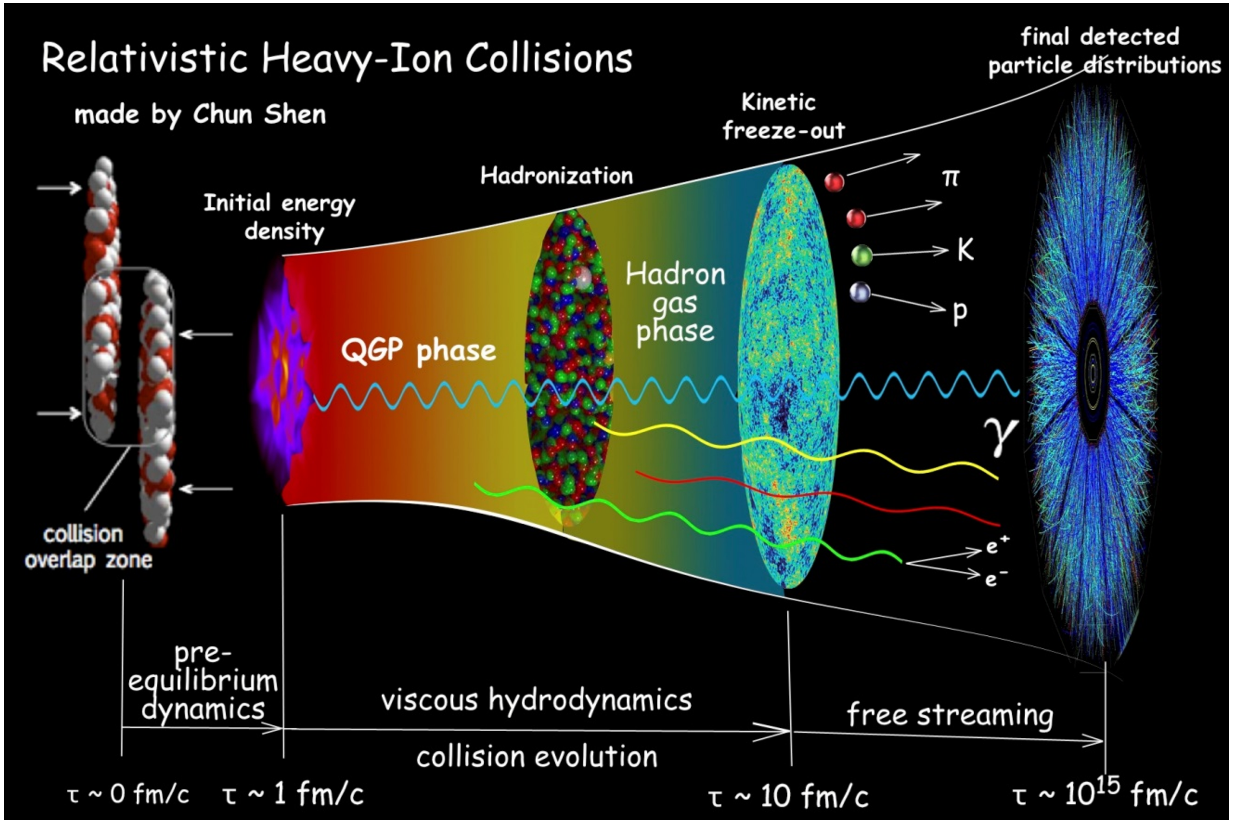

After a pre-equilibrium stage the system evolution can be described in terms of viscous hydrodynamics (QGP properties similar to those of a strongly interacting fluid)

- Initial hot and dense partonic matter rapidly expands.
- Collective flow develops and the system cools down.
- Phase transition (crossover) to hadron gas takes place at $T_{(pseudo-)critical}$.
- Chemical freeze-out takes place when inelastic collisions stop.
- Kinetic freeze-out happens after the chemical freeze-out once elastic collisions stop.

Light flavour hadrons

The production of particles formed only by light quarks (u, d, s), as π, K, p, Λ, Ξ, Ω , $K^*(892)^0$, $\phi(1020)$ and d, (anti-)nuclei (^3He, ^4He) and $^3_\Lambda H$, at low and intermediate p_T, allow us to

- Constrain the soft particle production models
- Check strangeness production mechanisms (no net strangeness is present in colliding nuclei)
- Study collective phenomena characterizing the dynamical evolution of the fireball
- Probe the thermal models for particles production
- Test nuclei production mechanisms
- Understand the late hadronic phase (K*, see talk by A. Knospe)

The ALICE detector

ALICE particle identification capabilities are unique.
Almost all known techniques are exploited: dE/dx, time-of-flight, transition radiation, Cherenkov radiation, calorimetry and decay topology (V0, cascade)

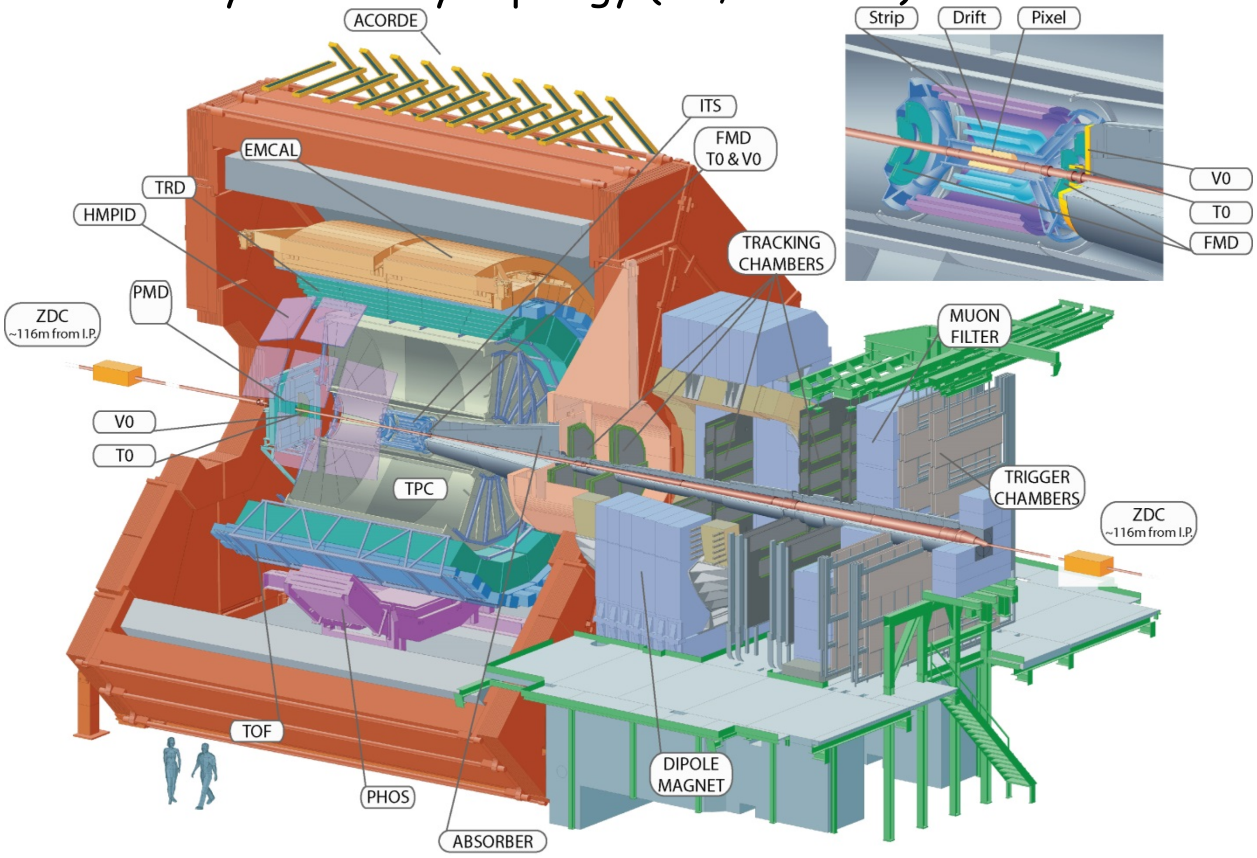

The ALICE detector

ALICE particle identification capabilities are unique. Almost all known techniques are exploited: dE/dx, time-of-flight, transition radiation, Cherenkov radiation, calorimetry and decay topology (V0, cascade)

ITS: particle identification via dE/dx and precise separation of primary particles and those from weak decays of strange particles or knock-out from material

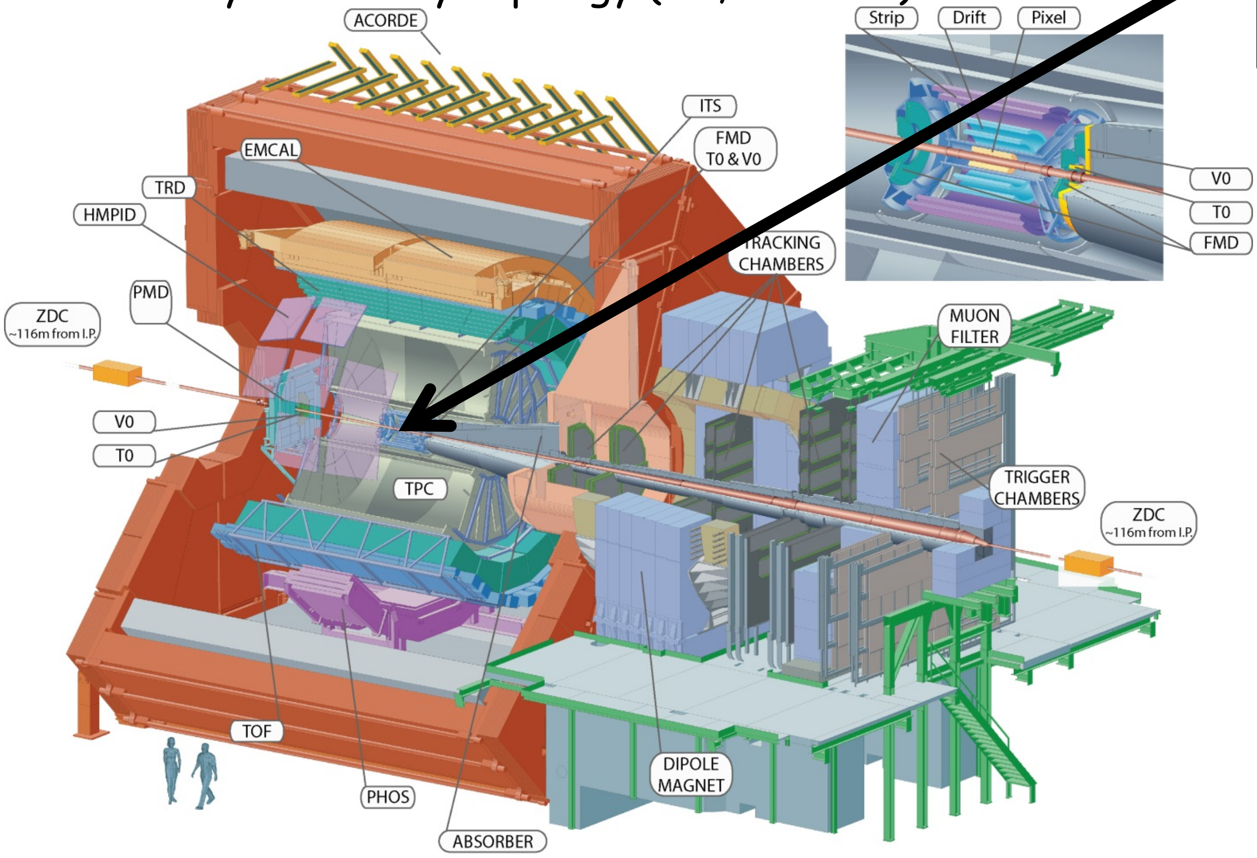

The ALICE detector

ITS: particle identification via dE/dx and precise separation of primary particles and those from weak decays of strange particles or knock-out from material

ALICE Coll. , Int. J. Mod. Phys. A29(2014)1430044

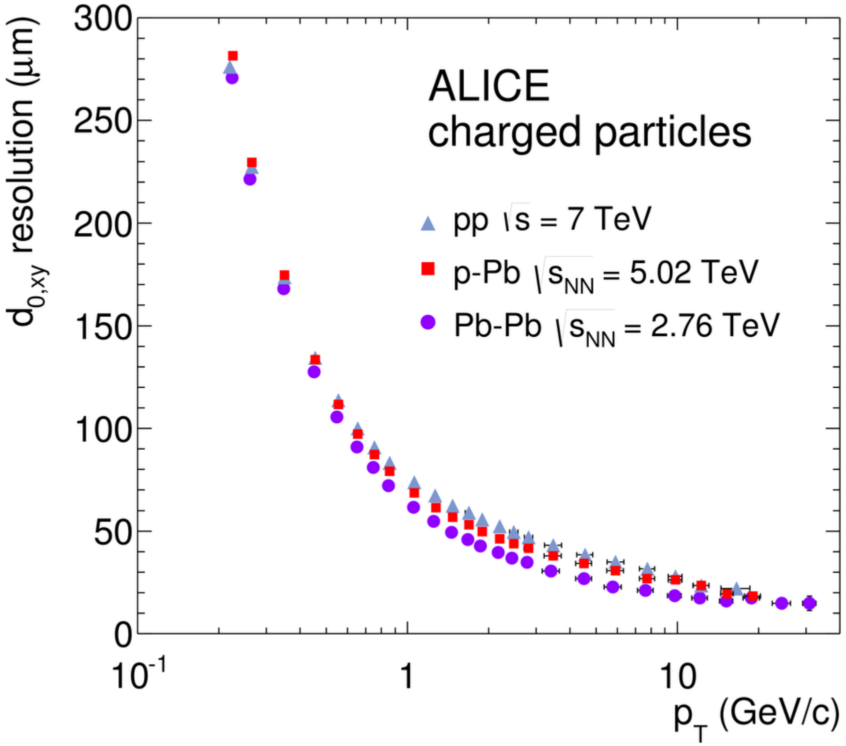

Resolution of the transverse distance < 50 μm for p_T>1 GeV/c

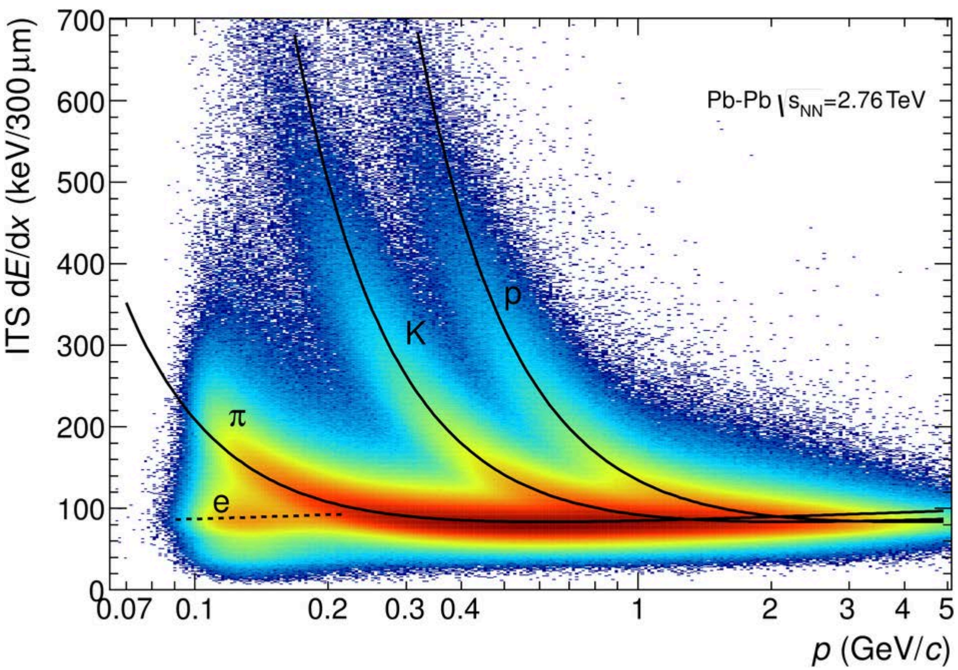

Energy-loss distribution in ITS-stand alone

The ALICE detector

ALICE particle identification capabilities are unique. Almost all known techniques are exploited: dE/dx, time-of-flight, transition radiation, Cherenkov radiation, calorimetry and decay topology (V0, cascade)

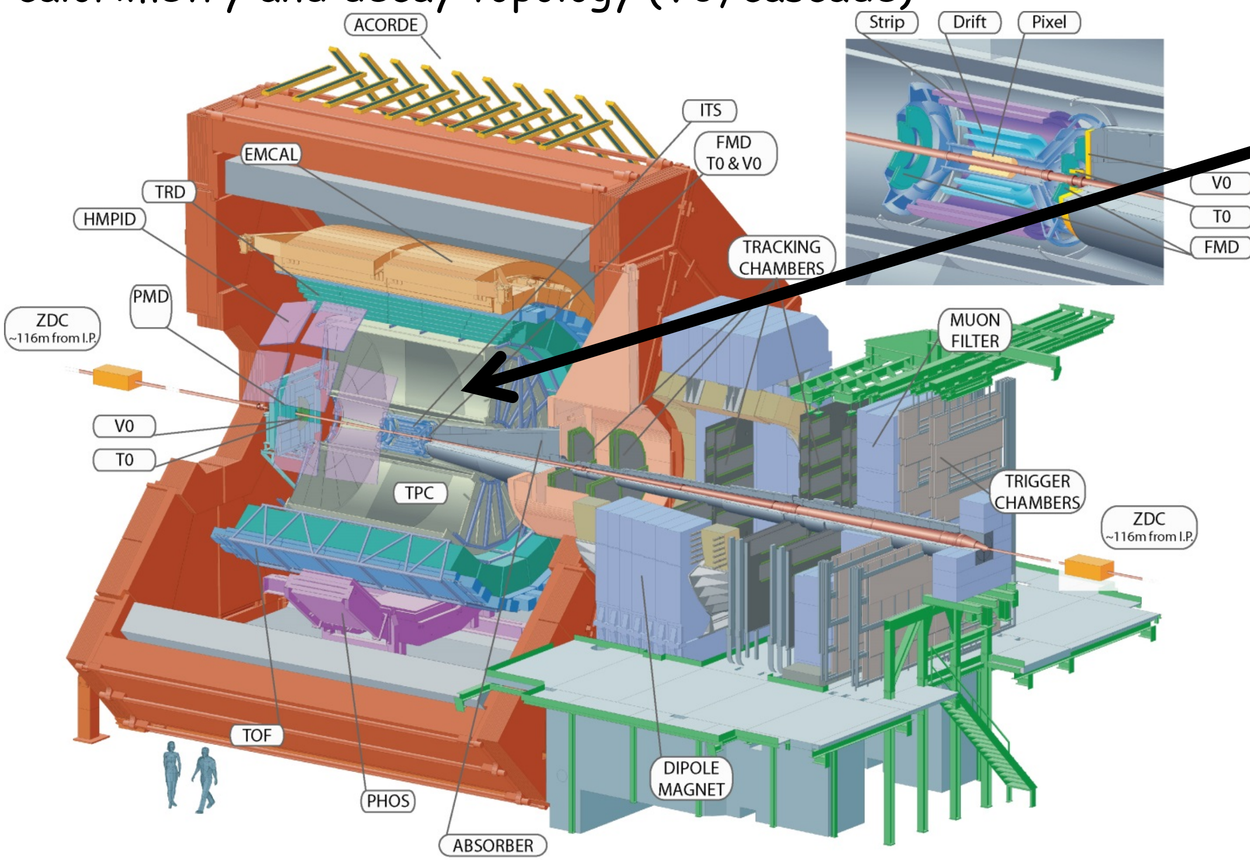

ITS: particle identification via dE/dx and precise separation of primary particles and those from weak decays of strange particles or knock-out from material

TPC: particle identification via dE/dx

The ALICE detector

ITS: particle identification via dE/dx and precise separation of primary particles and those from weak decays of strange particles or knock-out from material

TPC: particle identification via dE/dx

ALICE Coll. , Int. J. Mod. Phys. A29(2014)1430044

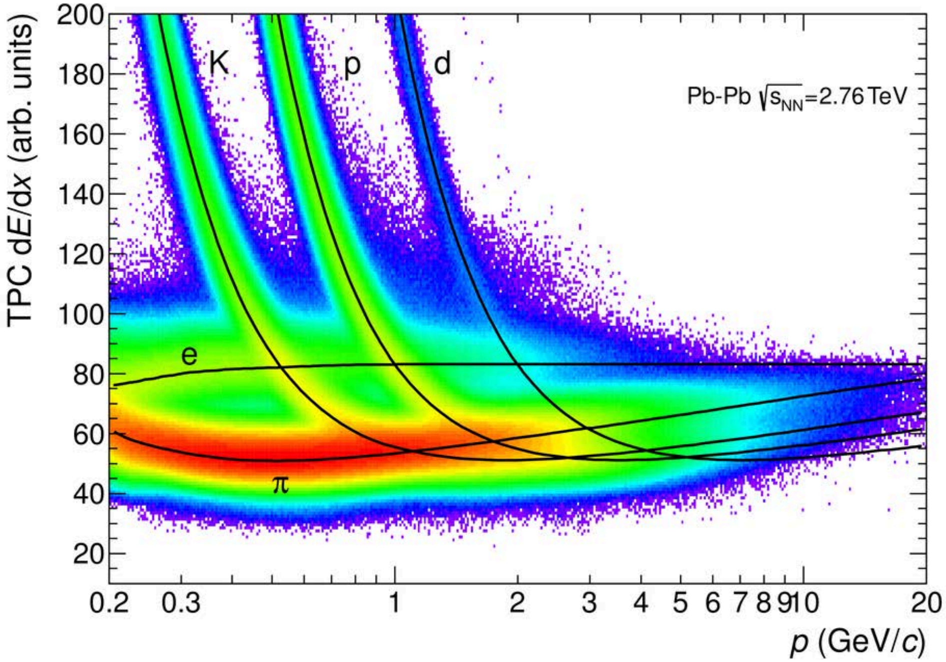

TPC specific energy loss vs. particle momentum

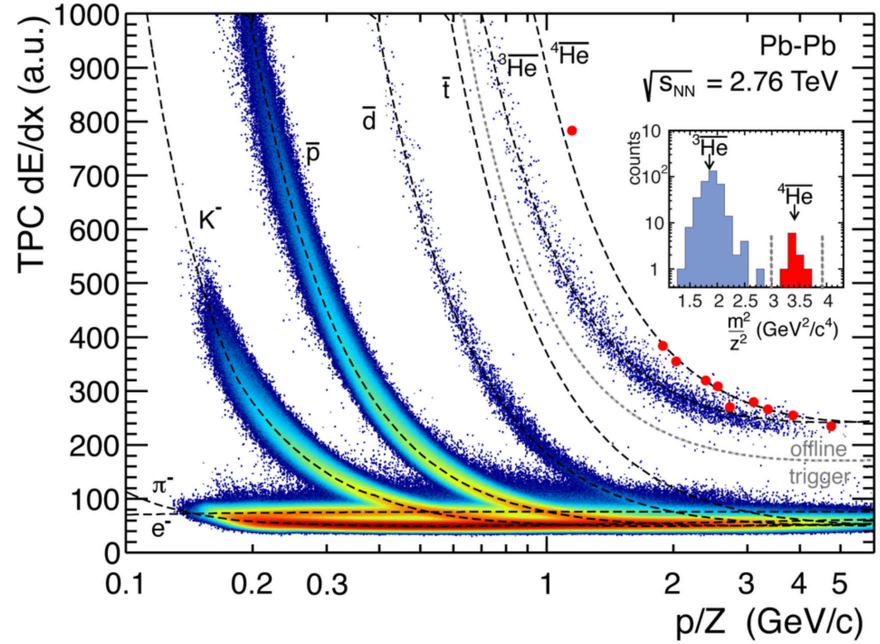

dE/dx vs. p/Z for negatively-charged particles

The ALICE detector

ALICE particle identification capabilities are unique.
Almost all known techniques are exploited: dE/dx, time-of-flight, transition radiation, Cherenkov radiation, calorimetry and decay topology (V0, cascade)

ITS: particle identification via dE/dx and precise separation of primary particles and those from weak decays of strange particles or knock-out from material

TPC: particle identification via dE/dx

TOF: particle identification via time-of-flight

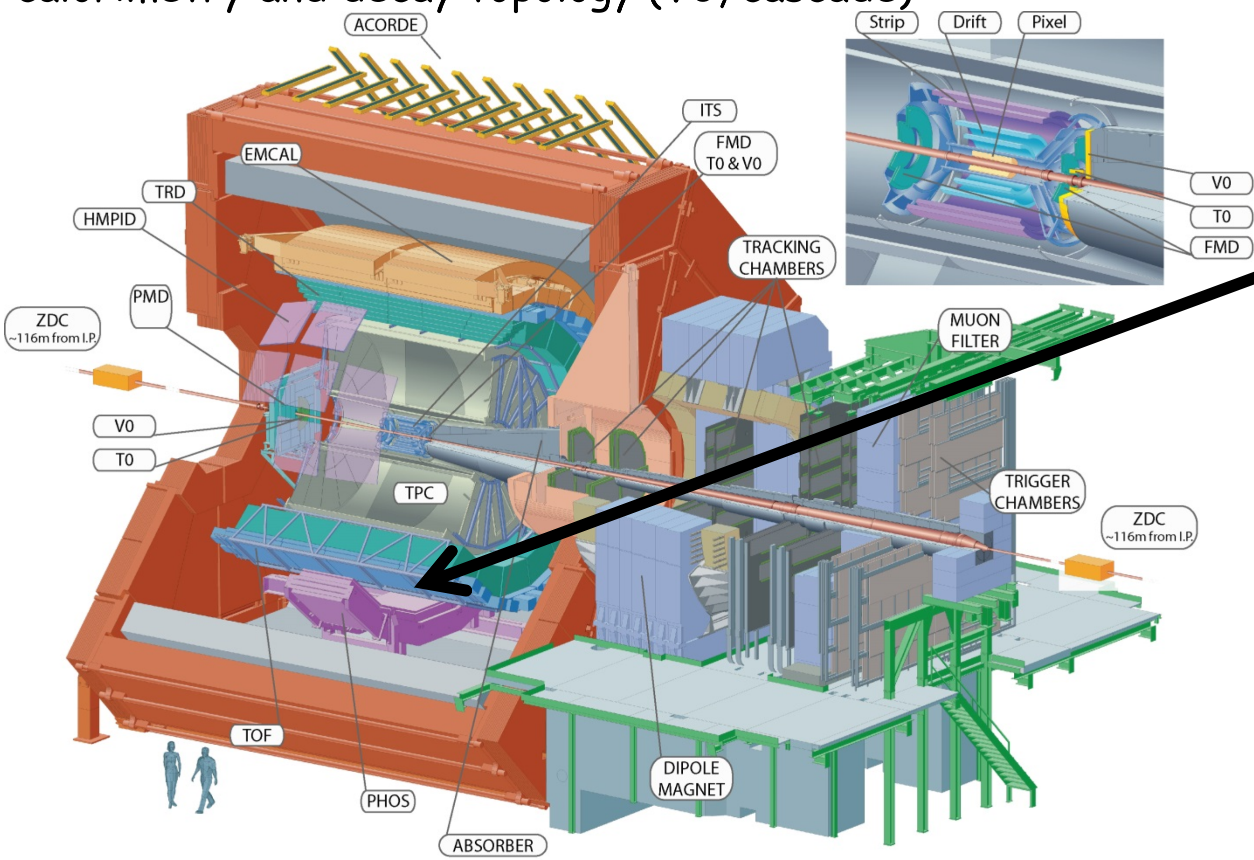

The ALICE detector

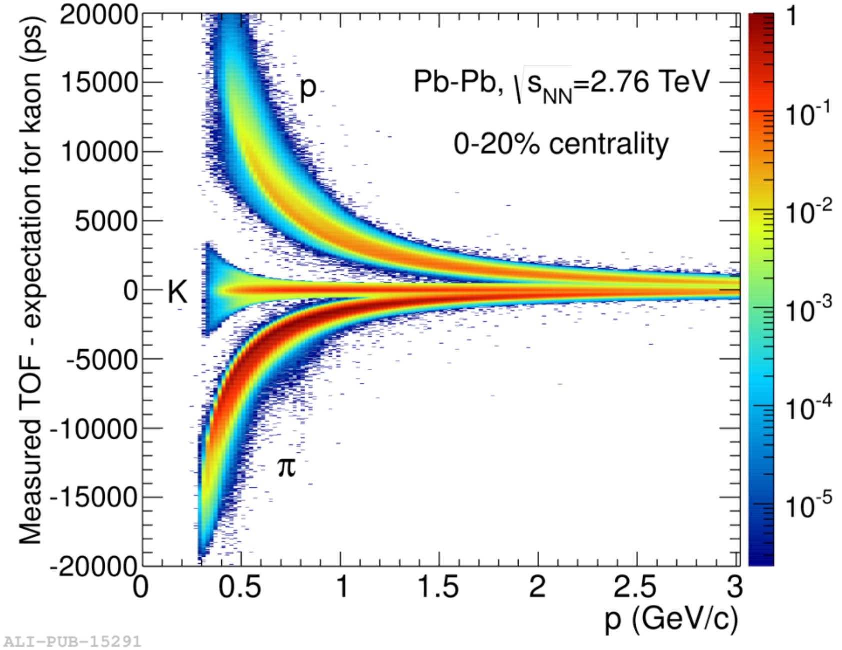

ALICE Coll. , Int. J. Mod. Phys. A29(2014)1430044

ITS: particle identification via dE/dx and precise separation of primary particles and those from weak decays of strange particles or knock-out from material

TPC: particle identification via dE/dx

TOF: particle identification via time-of-flight

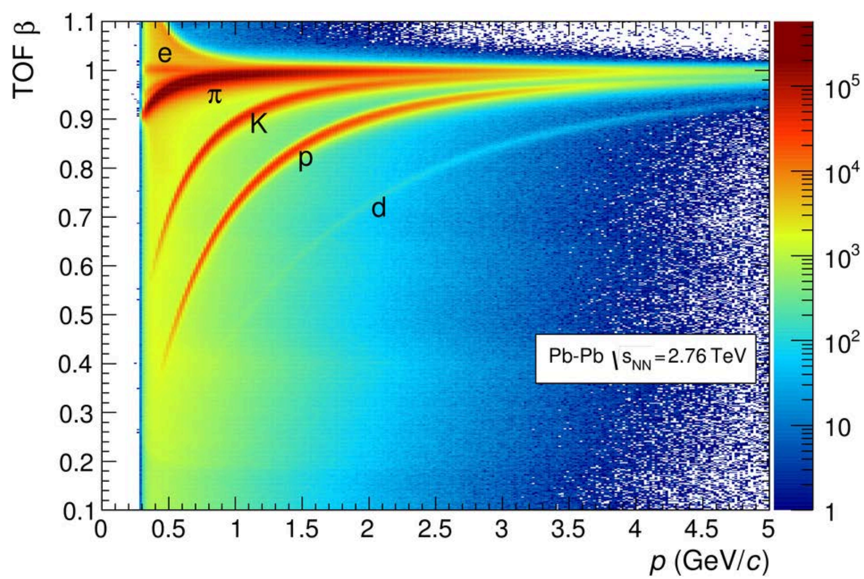

The ALICE detector

ALICE particle identification capabilities are unique. Almost all known techniques are exploited: dE/dx, time-of-flight, transition radiation, Cherenkov radiation, calorimetry and decay topology (V0, cascade)

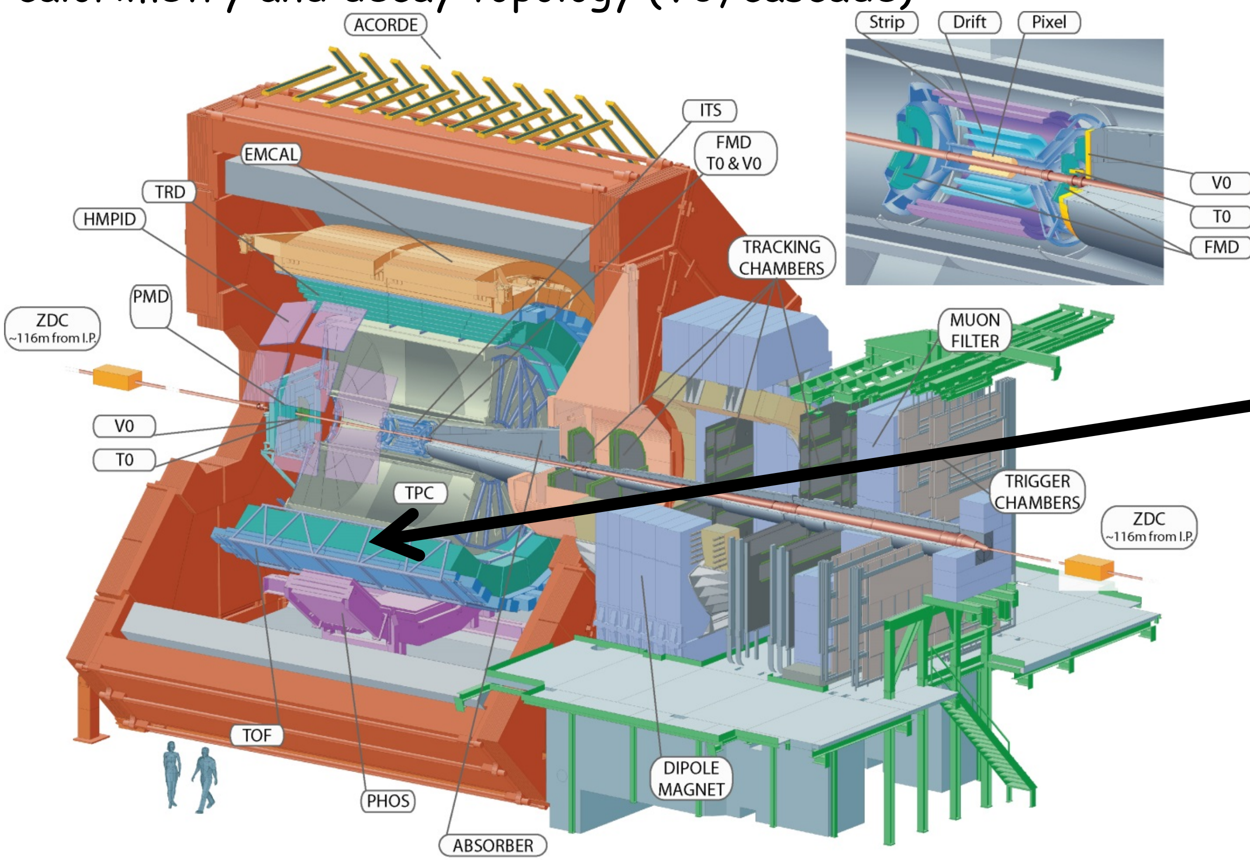

ITS: particle identification via dE/dx and precise separation of primary particles and those from weak decays of strange particles or knock-out from material

TPC: particle identification via dE/dx

TOF: particle identification via time-of-flight

TRD: electron identification via transition radiation

The ALICE detector

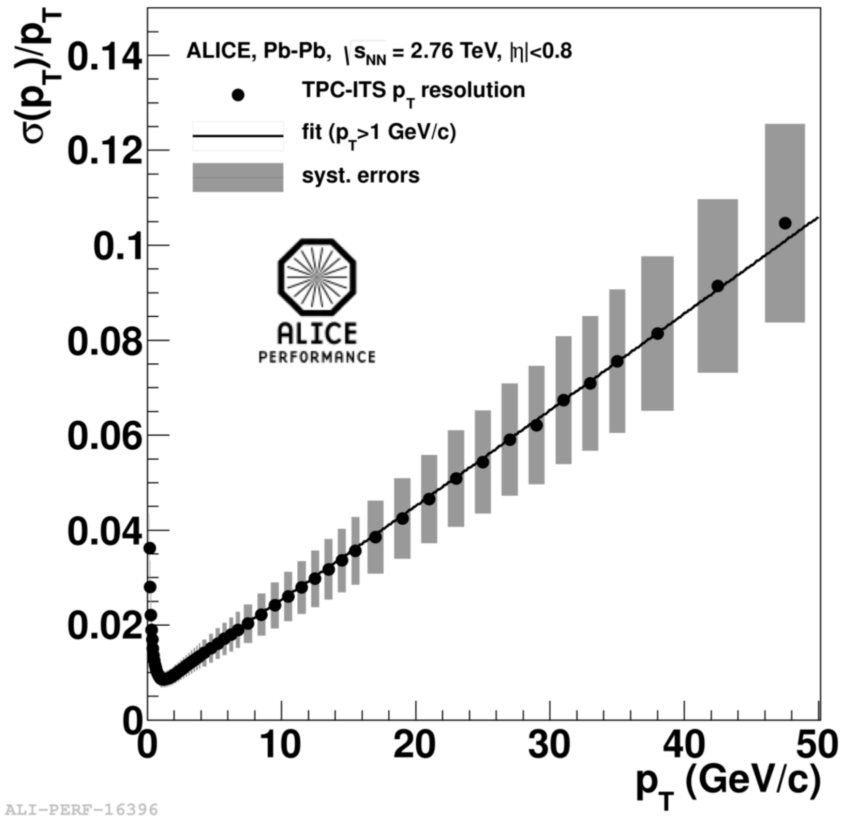

Relative p_T resolution

ITS: particle identification via dE/dx and precise separation of primary particles and those from weak decays of strange particles or knock-out from material

TPC: particle identfication via dE/dx

TOF: particle identification via time-of-flight

TRD: electron identification via transition radiation

ITS+TPC+(TRD): excellent track reconstruction capabilities in a high track density environment

The ALICE detector

ALICE particle identification capabilities are unique.
Almost all known techniques are exploited: dE/dx, time-of-flight, transition radiation, Cherenkov radiation, calorimetry and decay topology (V0, cascade)

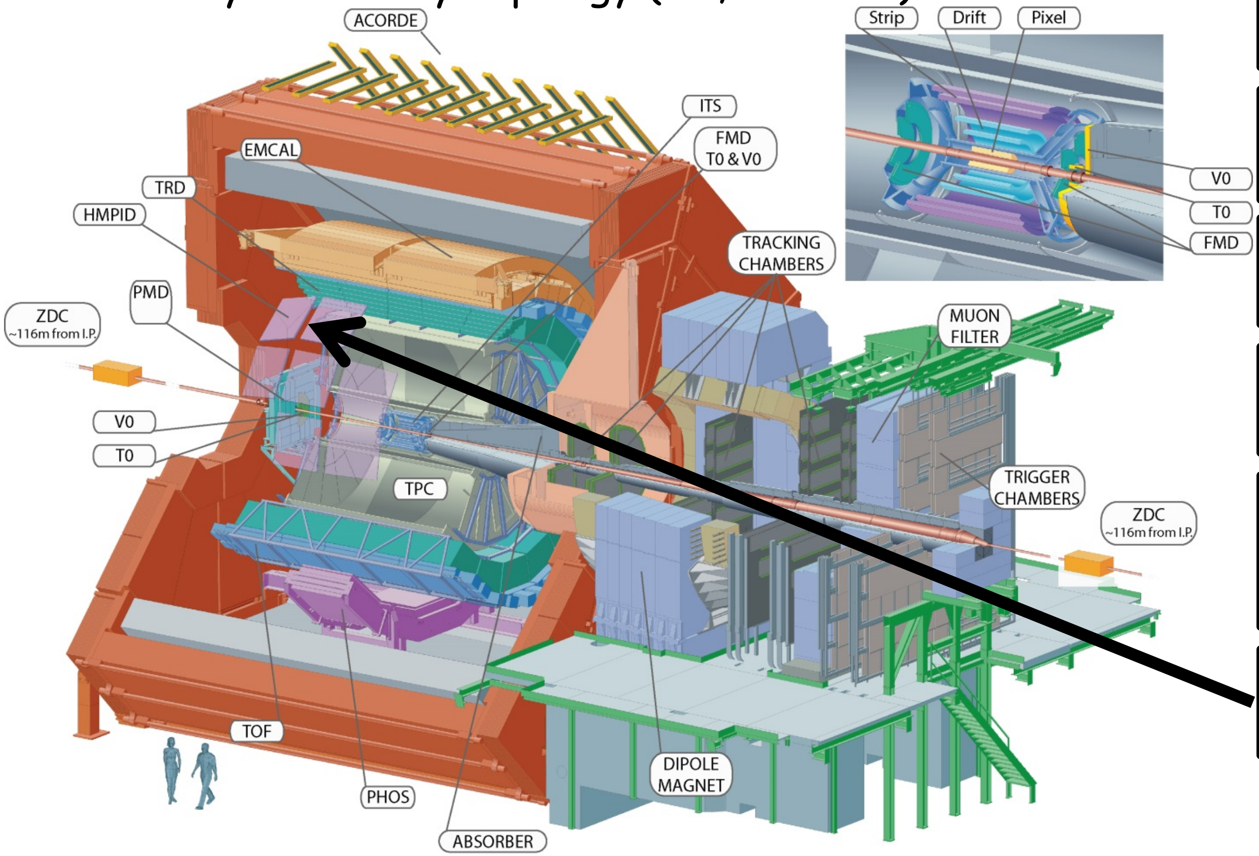

ITS: particle identification via dE/dx and precise separation of primary particles and those from weak decays of strange particles or knock-out from material

TPC: particle identification via dE/dx

TOF: particle identification via time-of-flight

TRD: electron identification via transition radiation

ITS+TPC+TRD: excellent track reconstruction capabilities in a high track density environment

HMPID: particle identification via Cherenkov radiation

The ALICE detector

ALICE particle identification capabilities are unique.
Almost all known techniques are exploited: dE/dx, time-of-flight, transition radiation, Cherenkov radiation, calorimetry and decay topology (V0, cascade)

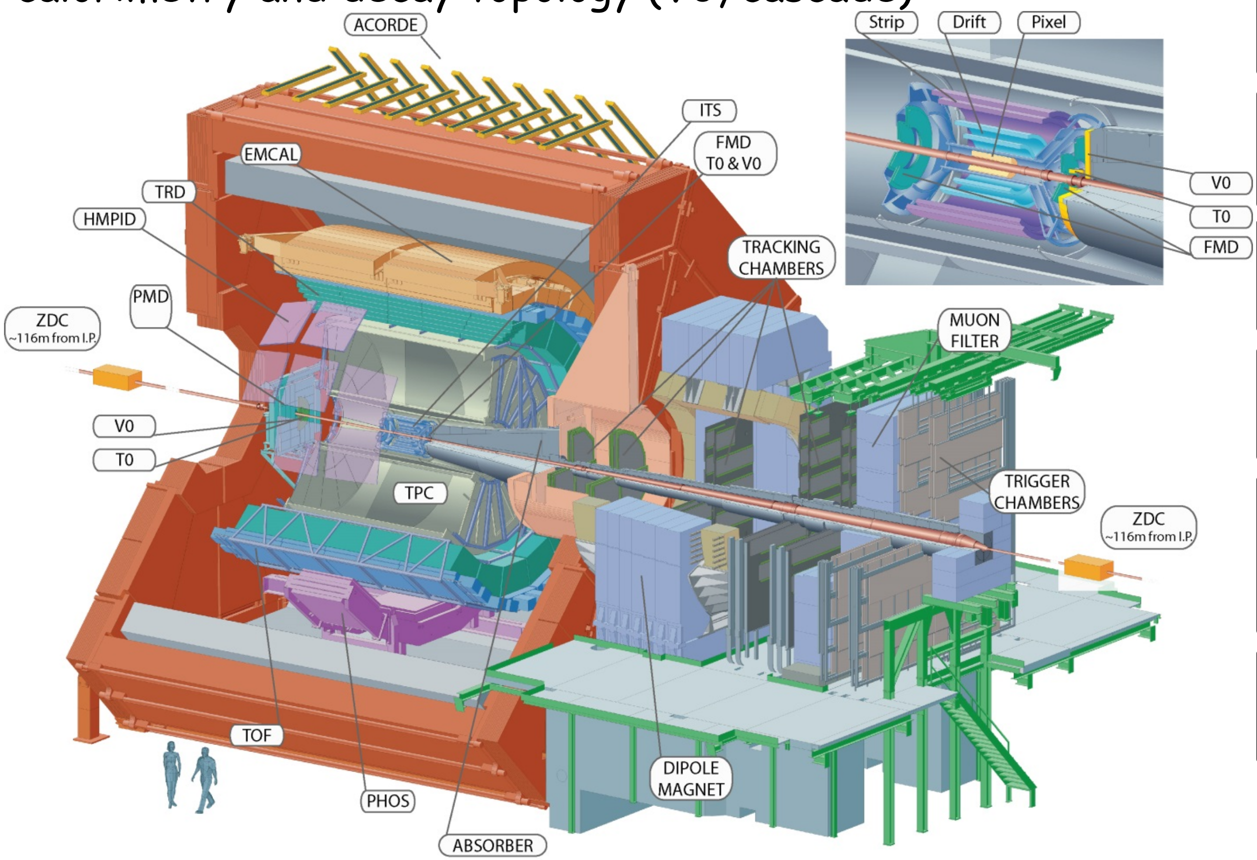

ITS: particle identification via dE/dx and precise separation of primary particles and those from weak decays of strange particles or knock-out from material

TPC: particle identification via dE/dx

TOF: particle identification via time-of-flight

TRD: electron identification via transition radiation

ITS+TPC+TRD: excellent track reconstruction capabilities in a high track density environment

HMPID: particle identification via Cherenkov radiation

Particle identification over a wide momentum range (0.1 GeV/c to ≈ 30 GeV/c)
→ ALICE is ideally suited for the measurement of light flavour hadrons

$K^0_S, \Lambda, \Xi, \Omega, {}^3_\Lambda H$

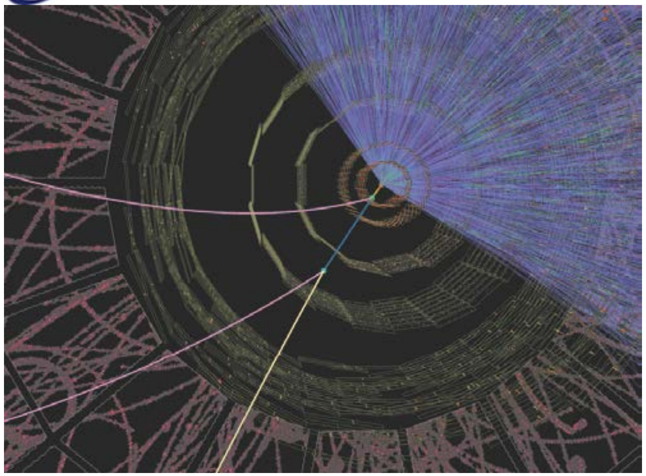

Weakly decaying hadrons and hypernuclei are reconstructed via their decay topology by combining their daughter tracks which are displaced from the primary vertex

Single-strange

$K^0_S(d\bar{s}) \rightarrow \pi^+\pi^-$

$\Lambda(uds) \rightarrow p\pi^-$

$\overline{\Lambda}(\overline{uds}) \rightarrow \bar{p}\pi^+$

Multi-strange

$\Xi^-(dss) \rightarrow \Lambda\pi^- \rightarrow p\pi^-\pi^-$

$\overline{\Xi}^+(\overline{dss}) \rightarrow \overline{\Lambda}\pi^+ \rightarrow \bar{p}\pi^+\pi^+$

$\Omega^-(sss) \rightarrow \Lambda K^- \rightarrow p\pi^- K^-$

$\overline{\Omega}^+(\overline{sss}) \rightarrow \overline{\Lambda}K^+ \rightarrow \bar{p}\pi^+ K^+$

Hypernuclei

${}^3_\Lambda H \rightarrow {}^3He + \pi^-$

${}^3_\Lambda \overline{H} \rightarrow {}^3\overline{He} + \pi^+$

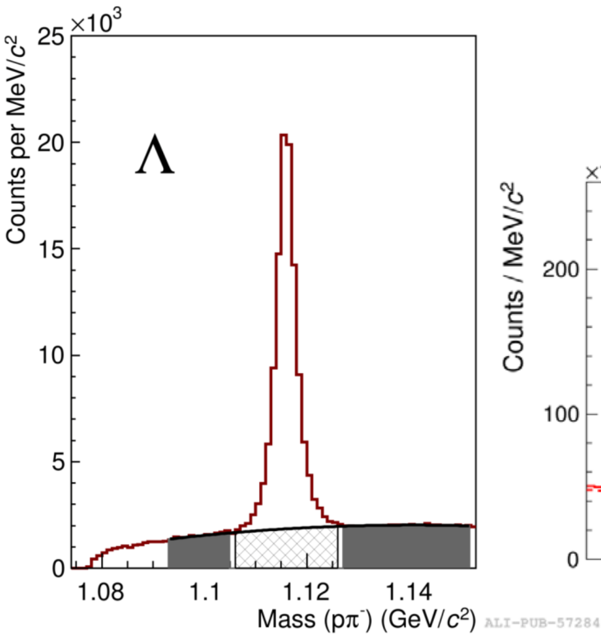

ALICE Coll. PRL 111, 222301 (2013)

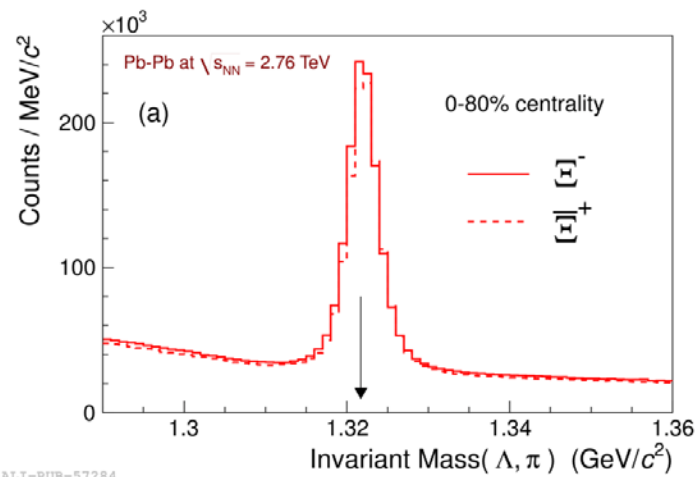

ALICE Coll. PL B728, 216 (2014)

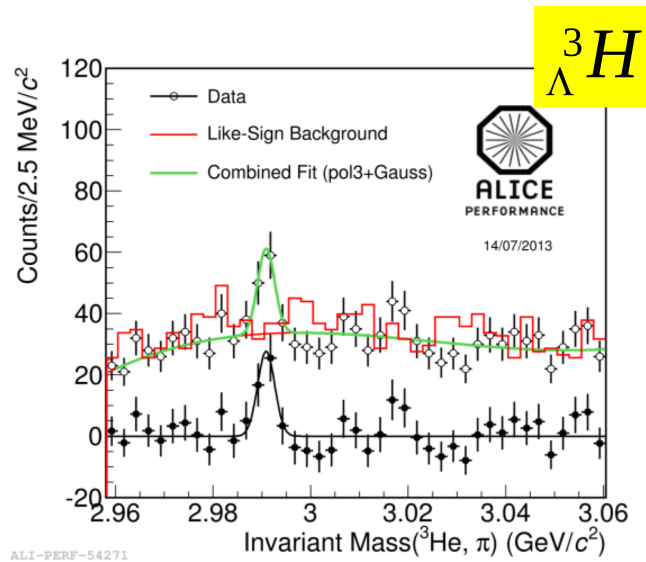

Resonances: $\phi(1020)$ and $K^*(892)^0$

- Combination of primary tracks after track-by-track particle identification
- The signal sits on a large combinatorial background (expecially in Pb-Pb collisions). The background is estimated by like-sign or event mixing technique

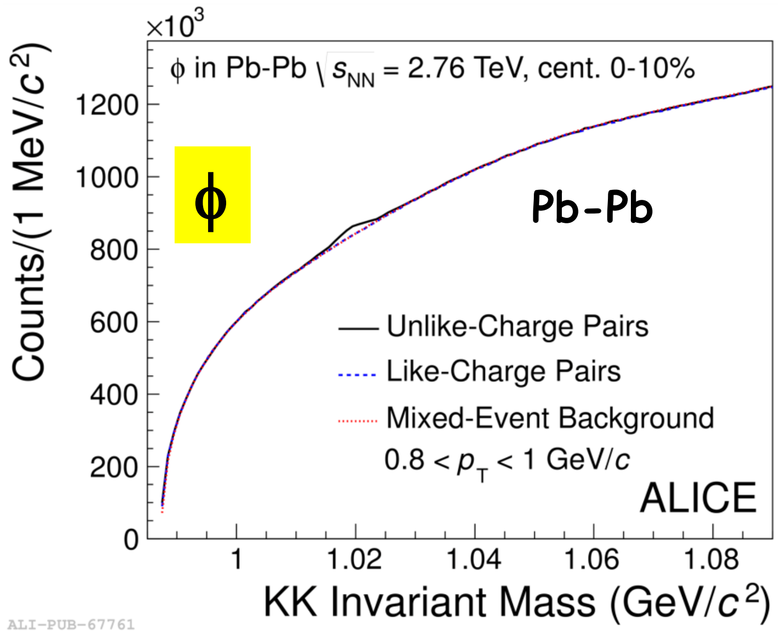

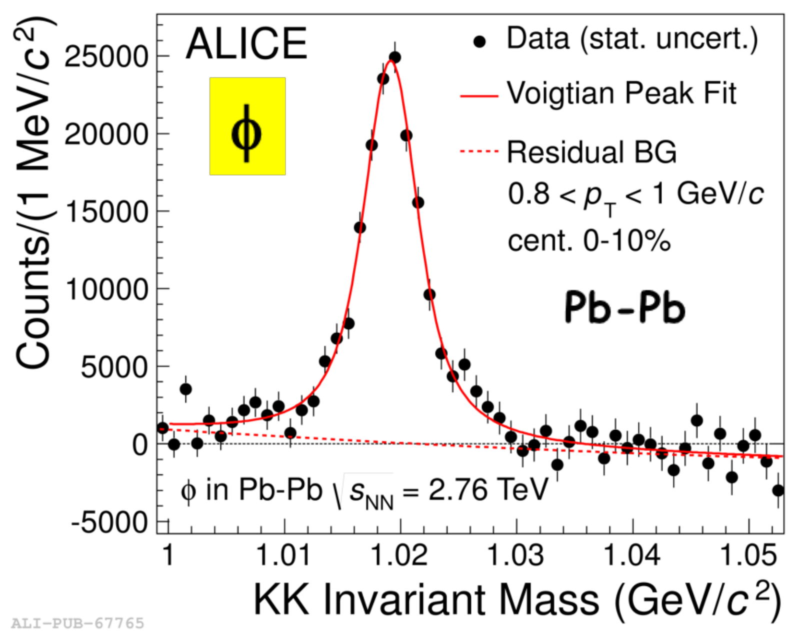

A. Knospe talk

ALICE Coll. Phys. Rev. C91(2015) 024609

Pb-Pb: Bulk particle production

ALICE coll. Phys. Rev. C88, 044910(2013)

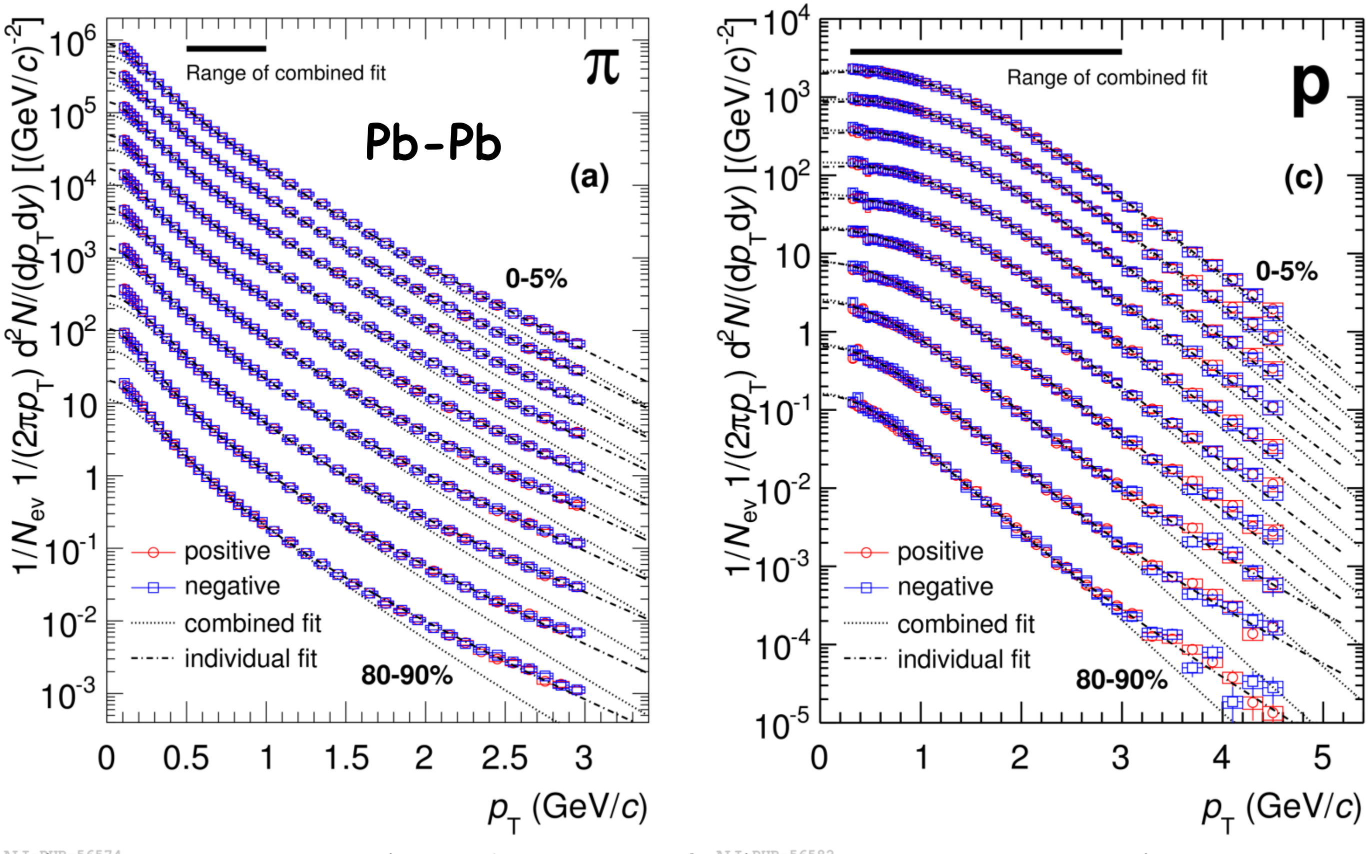

Clear signature of radial flow in Pb-Pb collisions

Characteristic hardening of the spectrum with increasing centrality.
It is more pronunced for heavier protons than for pions. →
Mass ordering as expected from collective hydro expansion.

Pb-Pb: Bulk particle production

ALICE coll. Phys. Rev. C88, 044910(2013)

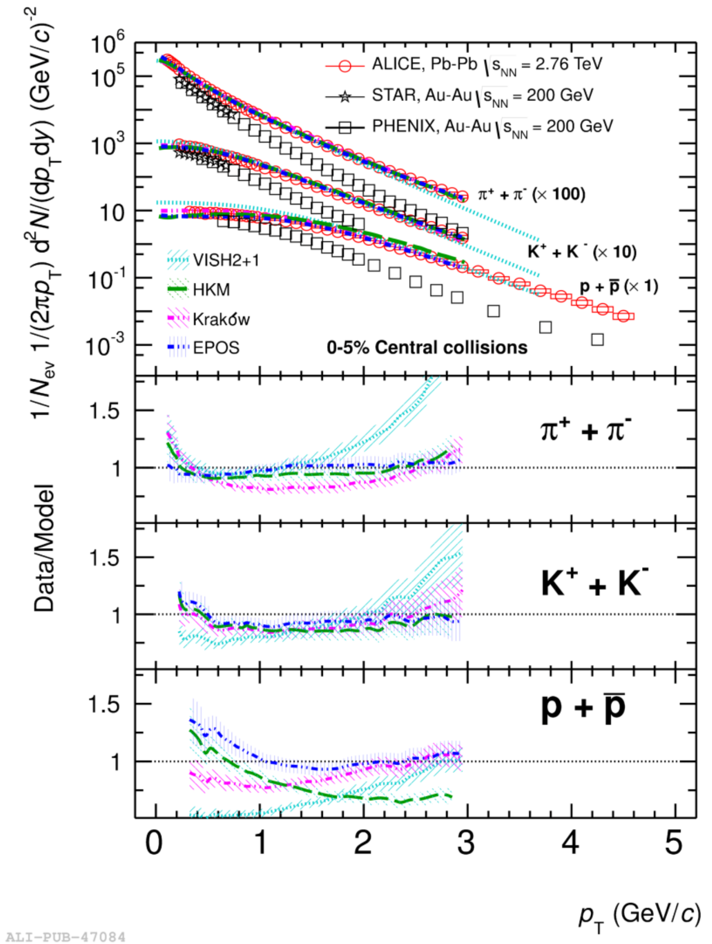

Stronger radial flow at LHC than at RHIC. From Blast-Wave fit:

T_{kin} ~ 95 MeV (~ RHIC value)

$\langle\beta_T\rangle$ ~ 0.65 c (~10% larger than RHIC)

HYDRO MODELS

- **VISH2+1**: viscous hydro
- **HKM**: ideal hydro with hadronic cascade following hydrodynamics (UrQMD)
- **Kraków**: hydro+ bulk viscous corrections
- **EPOS**: hydro+UrQMD, bulk +jets

Low p_T spectra nicely described by hydro models

Multi-strange hadron spectra in Pb-Pb

ALICE coll. PLB 728, 216 (2014)

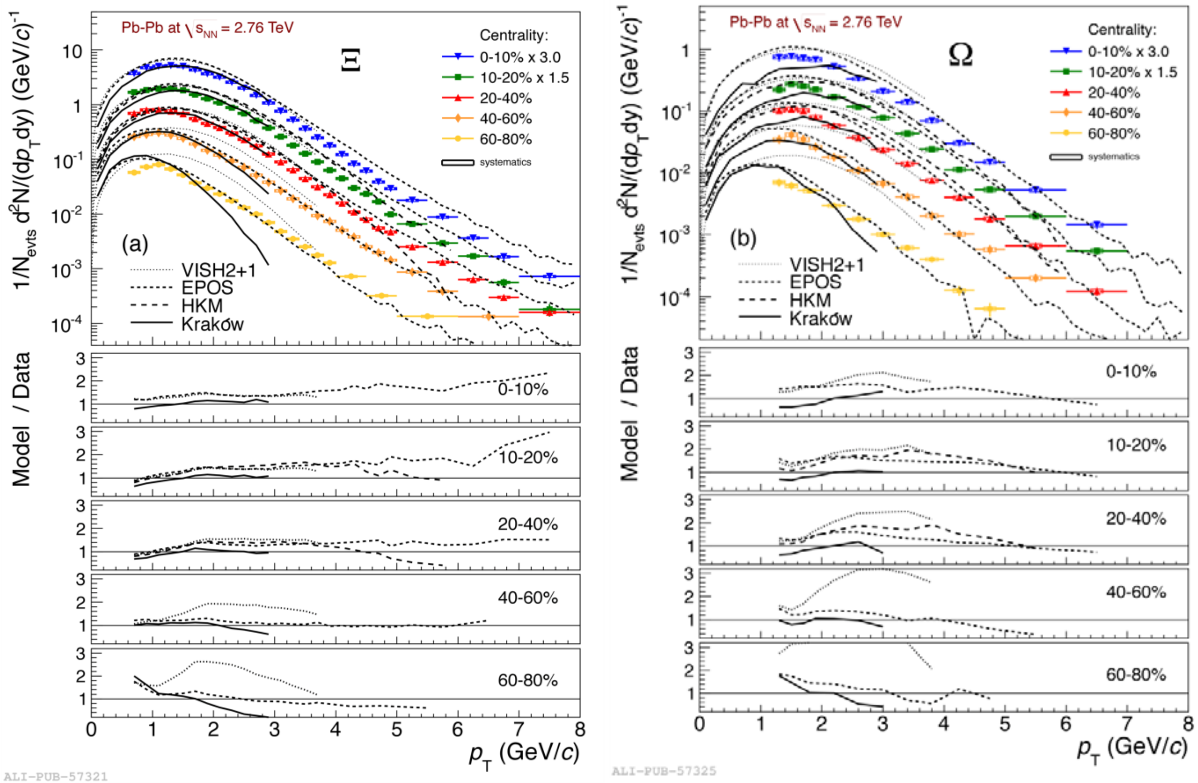

HYDRO MODELS

- **VISH2+1**: viscous hydro
- **HKM**: ideal hydro with hadronic cascade following hydrodynamics (UrQMD)
- **Kraków**: hydro+bulk viscous corrections
- **EPOS**: hydro+UrQMD, bulk+jets

Comparison to data:

- Kraków model best for yield and shape at $p_T < 3$ GeV/c
- EPOS reasonably good in a wider p_T range and vs centrality

Hydro models give a reasonable description of spectral shapes. Worse agreement for the Ω

ϕ/p ratio: mass ordering in Pb-Pb

Mass ordering can be best validated by looking simultaneously at ϕ and proton spectra, due to their similar mass

A. Knospe talk

ALICE Coll. Phys. Rev. C91(2015) 024609

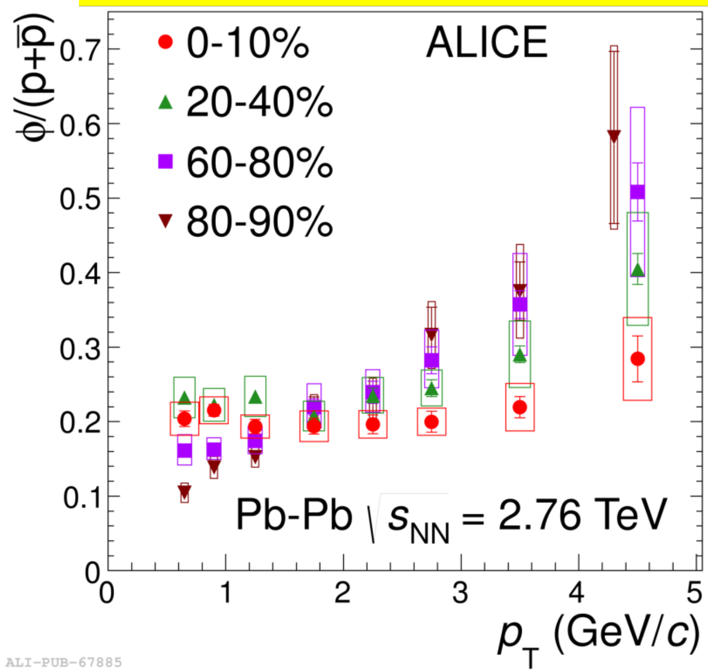

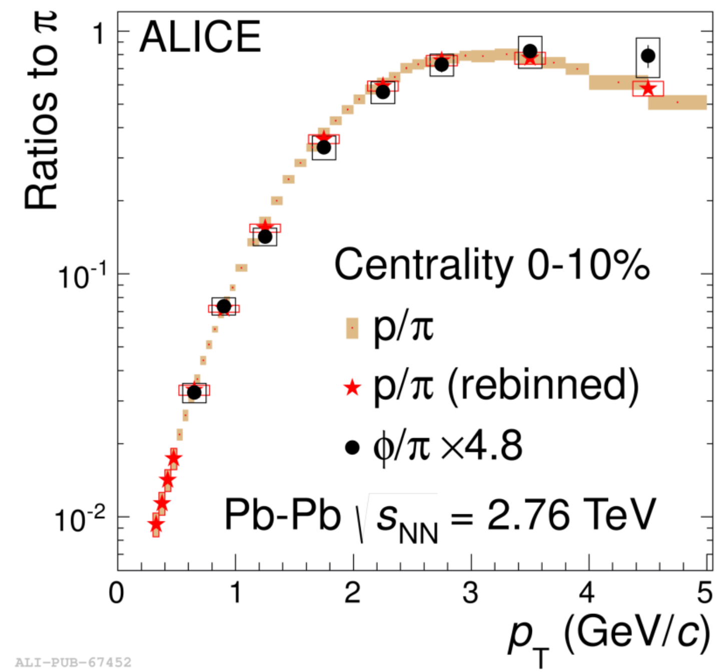

ϕ/p ratio is flat for p_T<3-4 GeV/c in central Pb-Pb collisions

ϕ-mesons and protons have p_T spectra with a similar shape

Low p_T spectral shape is determined by particle mass, i.e. consistent with hydrodynamic description

Model comparison for p-Pb collisions

ALICE coll. PLB 728, 25 (2014)

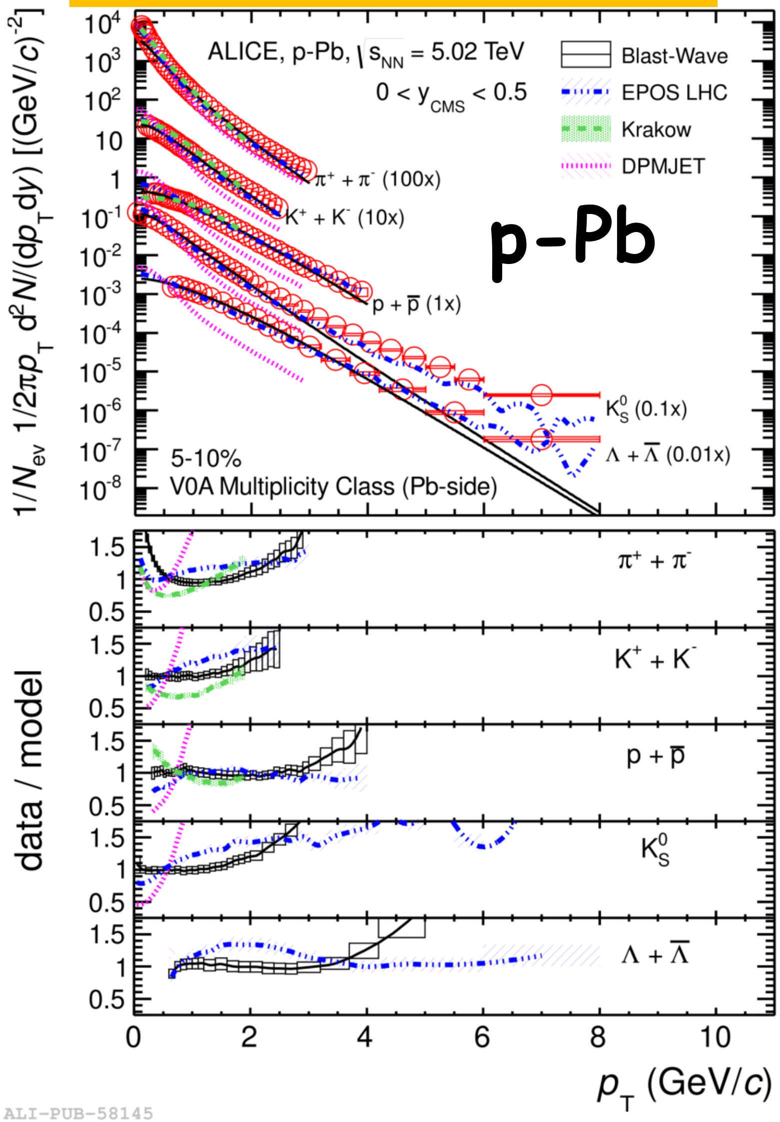

π

K

p

K^0_s

Λ

Blast-Wave: hydro-inspired fit, thermal sources expanding with common velocity

EPOS LHC: hydro +URQMD, bulk+jets

Kraków: hydro + bulk viscous corrections

DPMJET: pQCD inspired model

Hydrodynamic models (EPOS, Kraków) show a better agreement than QCD inspired models (DPMJET).

p-Pb and Pb-Pb data follow same trend, i.e. consistent with a collective expansion

Blast-wave fit in p-Pb collisions

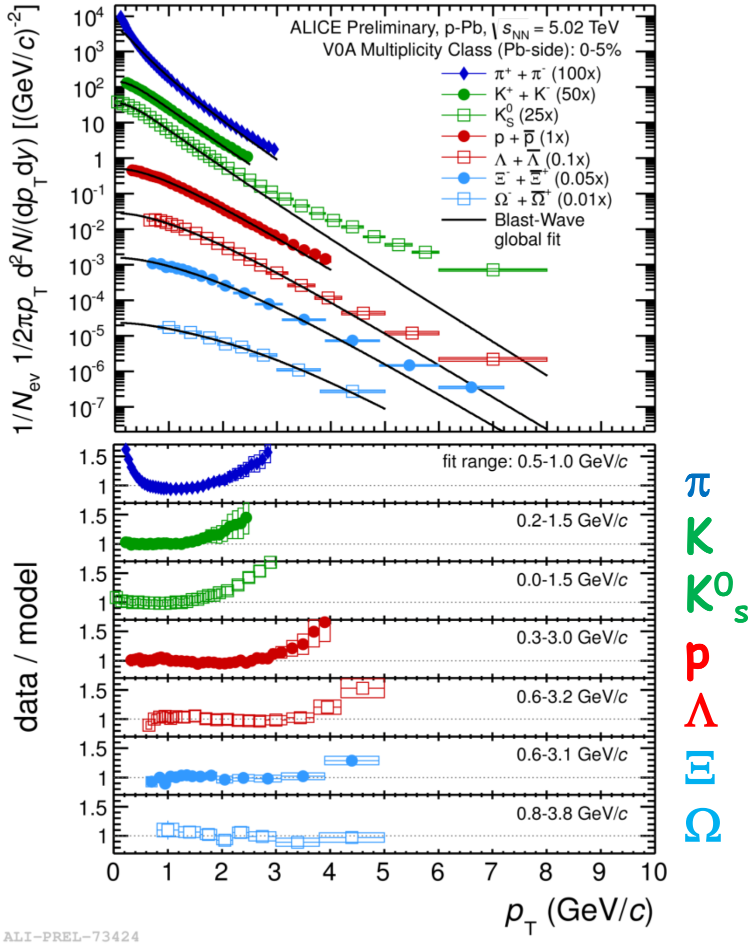

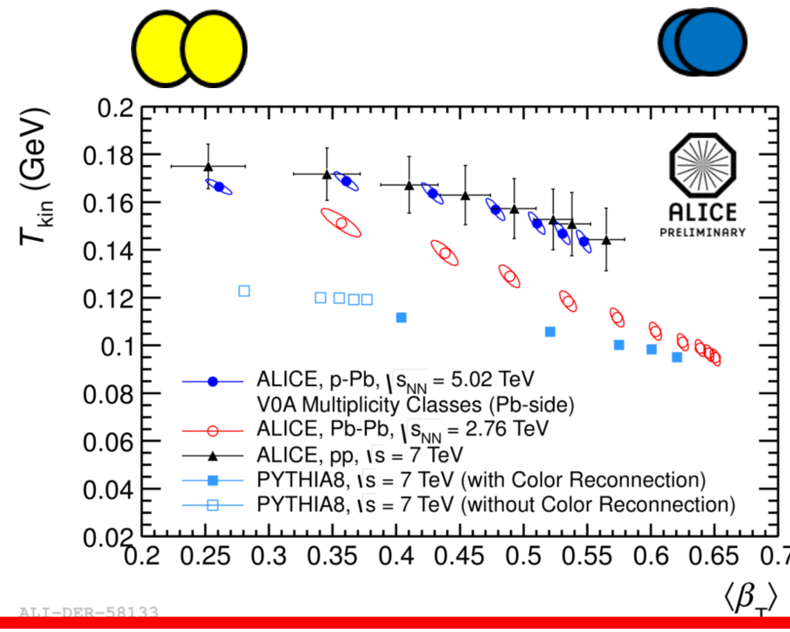

T_{kin} vs $\langle\beta_T\rangle$ for different multiplicity classes:

- Similar trend for Pb-Pb, p-Pb, pp
- Lower T_{kin} and higher radial flow in Pb-Pb
- PYTHIA 8 with color reconnection shows a similar trend (without hydrodynamic flow)

In p-Pb collisions a combined blast-wave fit to all particle data gives a reasonable description of low p_T spectra.

Other effects can mimic flow-like patterns!

Deuterons and ^3He in Pb-Pb

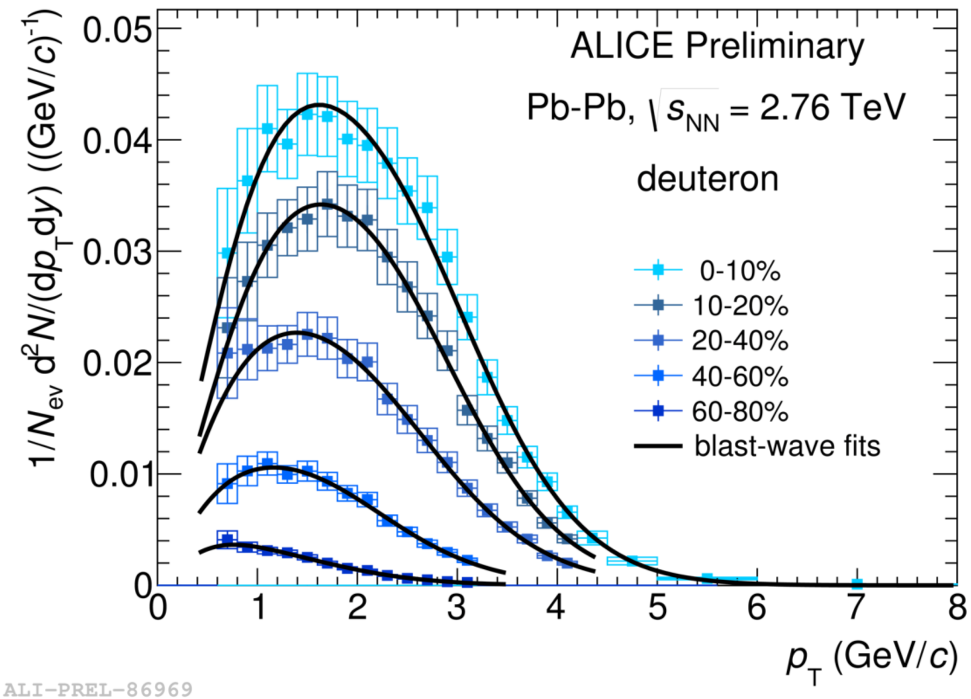

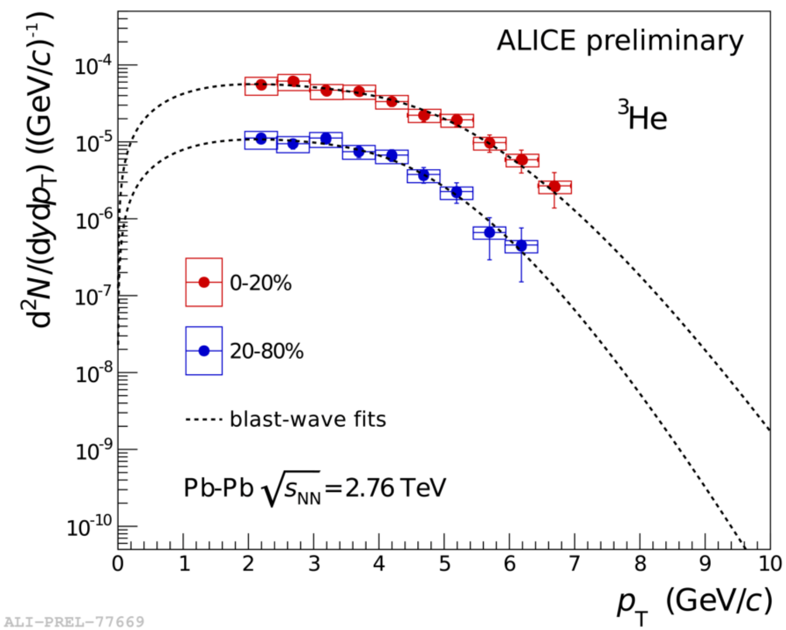

- Light (anti)nuclei are abundantly produced in heavy ion collisions.
- As expected in a hydrodynamic description of the fireball as a radially expanding source, a hardening of the spectrum with increasing centrality is observed.
- Blast wave fit was used for yield extraction in unmeasured p_T regions

Mass ordering in Pb-Pb

Anti-alpha production first observed at RHIC in heavy-ion collisions
(STAR coll., Nature 473, 353 (2011))

Anti-alpha dN/dy has been measured by ALICE in central Pb-Pb collisions at $\sqrt{s_{NN}}$ = 2.76 TeV.

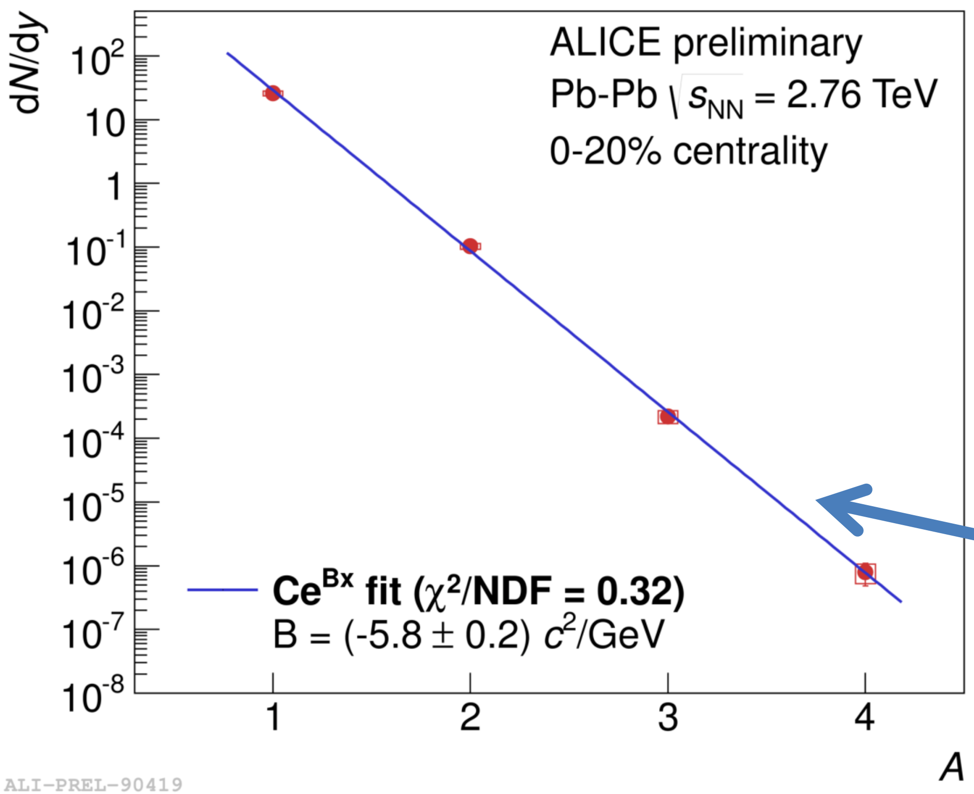

Thermal model prediction

$$\frac{dN}{dy} \propto \exp\left(-\frac{m}{T_{chem}}\right)$$

Nuclei follow nicely the exponential fall predicted by the model.
We get a penalty factor of ~ 300 for each added baryon

Hypertriton production and lifetime

The hypernucleus $^{3}_{\Lambda}H$ was measured by its weak decay in $^{3}He + \pi$ by the topological identification of secondary vertex + ^{3}He and π PID, with:

$\mu = 2.992 \pm 0.002$ GeV/c^2 (σ = $(2.08 \pm 0.50) \times 10^{-3}$ GeV/c^2) .

Agreement with literature value (Juric, Nucl. Phys. B52, 1(1973)):

$\mu = 2.99131 \pm 0.00005$ GeV/c^2

$^{3}_{\Lambda}H$ yield in agreement with thermal model T_{ch} = 156 MeV

Lifetime measured thanks to excellent determination of primary and decay vertex

$$N(t) = N(0)\exp\left[-\frac{t}{\tau}\right] = N(0)\exp\left(-\frac{L}{\beta\gamma c\tau}\right)$$

Where $t = L/(\beta\gamma c)$ and $\beta\gamma c = p/m$
With m the hypertriton mass, L the decay length and p the total momentum

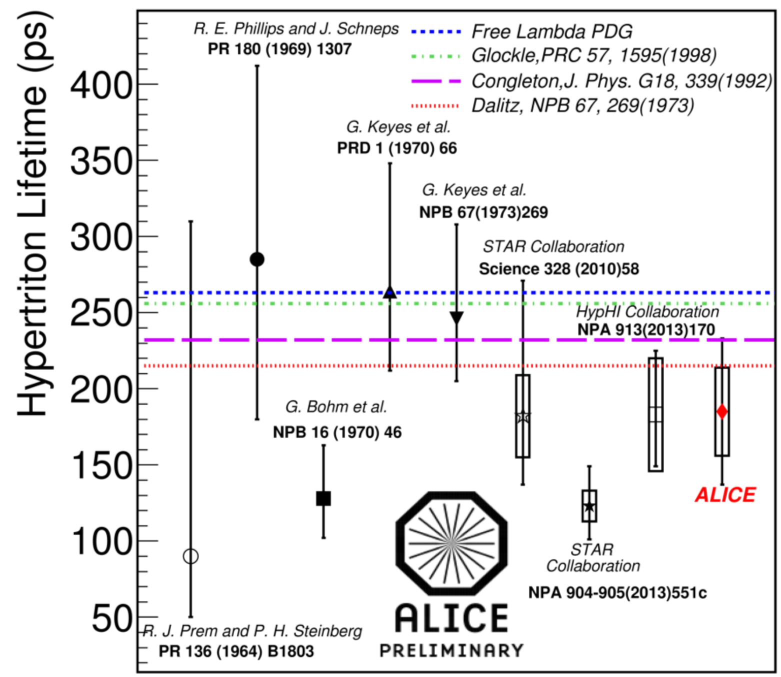

$c\tau$ = (5.5 ± 1.4 ± 0.68) cm
τ = 185 ±48 ±29 ps

Baryon-meson enhancement in p-Pb

Enhancement of baryon-meson ratios (Λ/K^0_S and p/π) in central A-A collisions vs. pp has been observed at LHC and RHIC energies. This is commonly understood in terms of collective flow/quark recombination.

ALICE coll. PLB 728, 25 (2014)

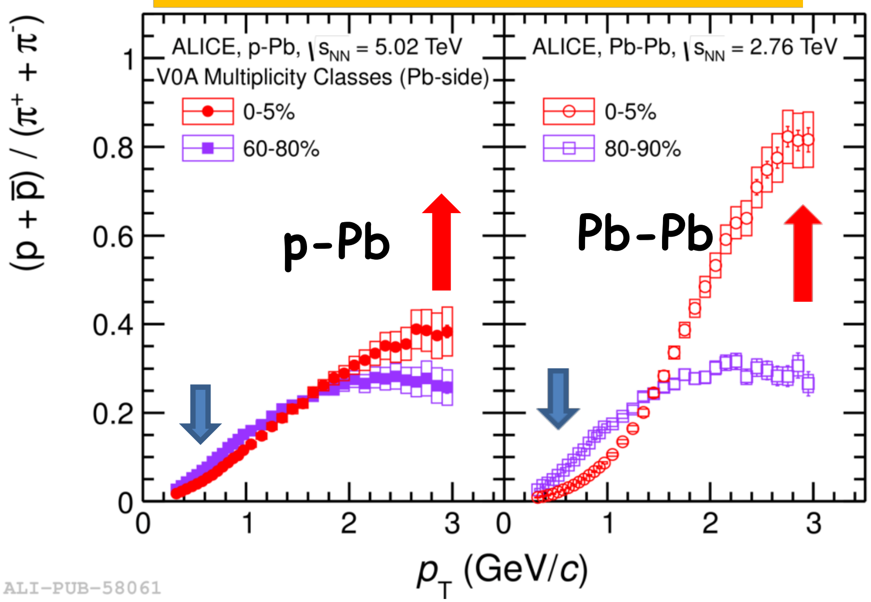

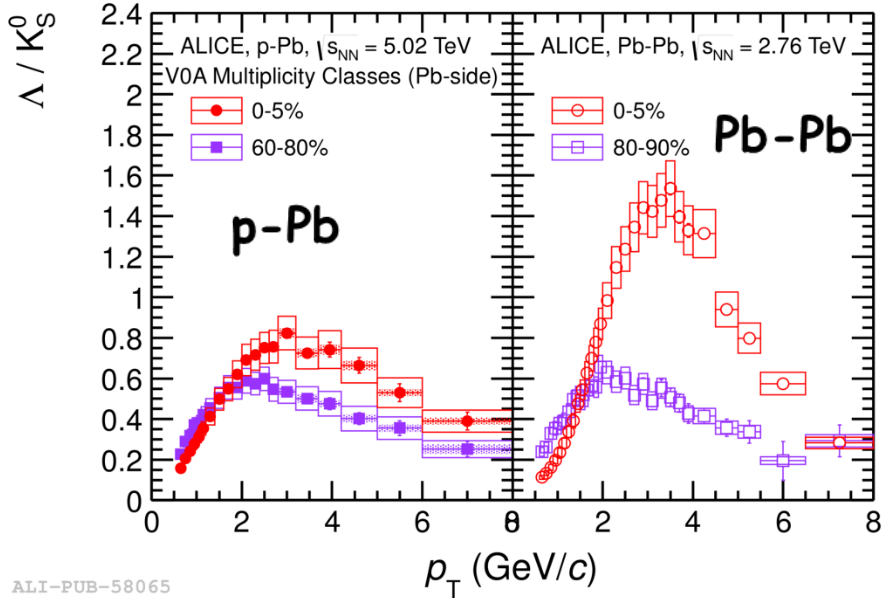

In p-Pb centrality/multiplicity dependence of the Λ/K^0_S and p/π ratios similar to Pb-Pb

- Enhancement at mid-p_T with increasing multiplicity
- Corresponding depletion in the low-p_T region

Λ/K^0_S ratio in jets in p-Pb

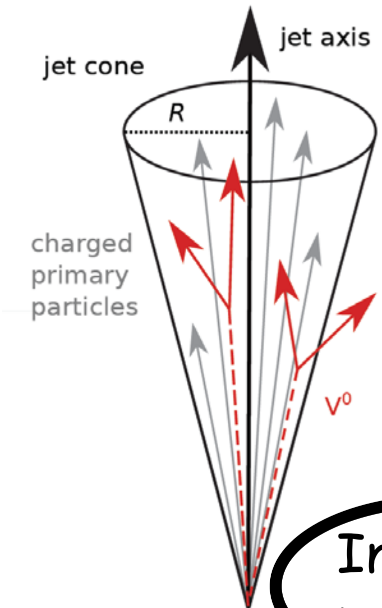

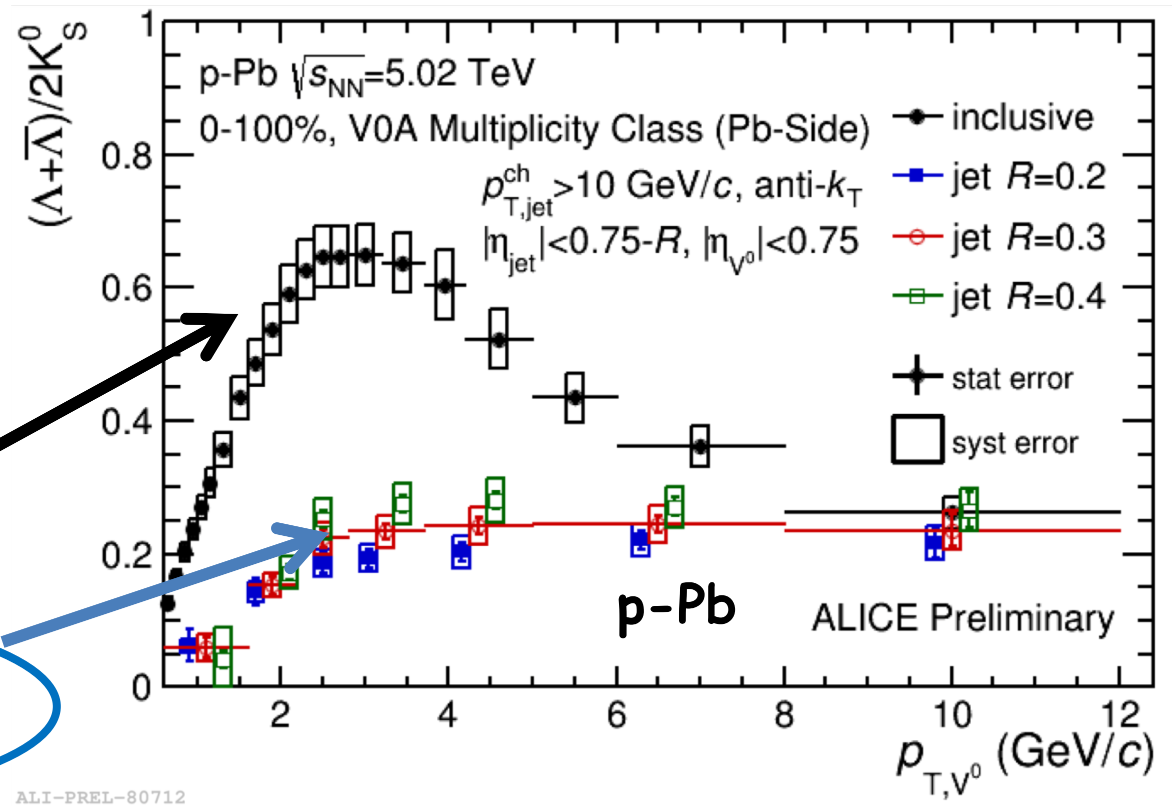

Inclusive particles

Particles in jets do not show enhancement

The extra baryons don't come from jets

Multi-strange to pion ratio in Pb-Pb

ALICE coll. PLB 728 (2014) 216

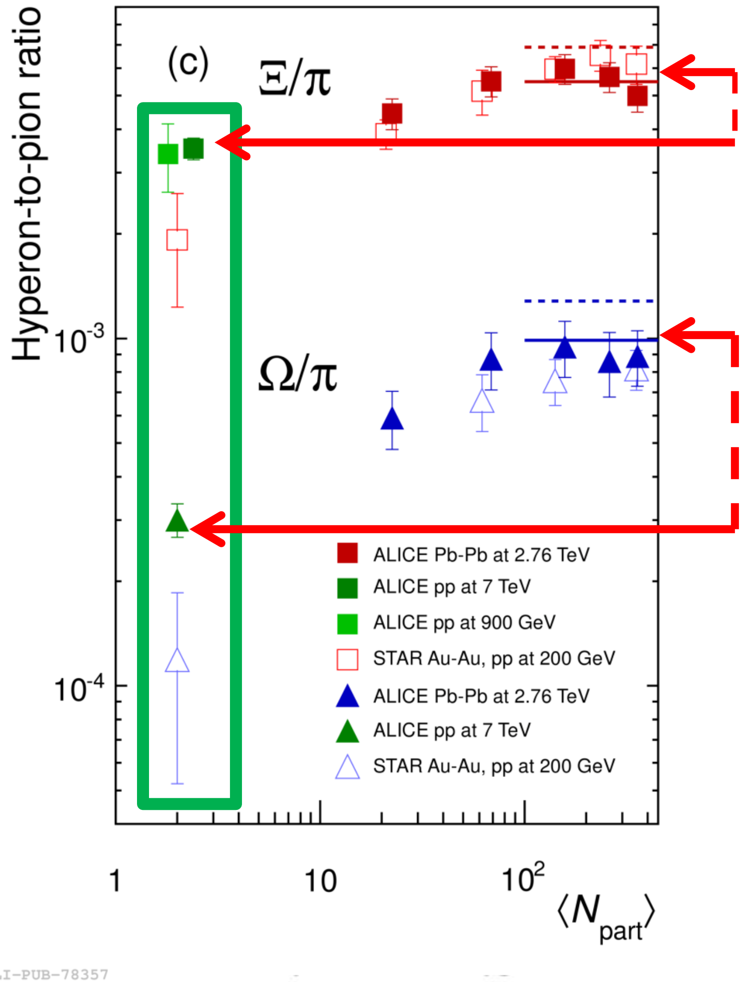

Strangeness enhancement

one of the first proposed QGP signatures

J. Rafelski et al., PRL 48 (1982)1066;

P. Koch et al., Phys. Rep. 142(1986)167

Relative production of strangeness in pp increases going from RHIC to LHC

Saturation of Ξ/π and Ω/π ratios for N_{part}>150. Ratios match prediction from thermal models based on a grand canonical approach (T_{fo}= 164 MeV (full line[1], 170 MeV (dashed line, [2])

Clear increase of strangeness production from pp to Pb-Pb

[1] A. Andronic et al. PLB 673(2009)142

[2] J. Cleymans et al., PRC 74 (2006) 034903

System size dependence

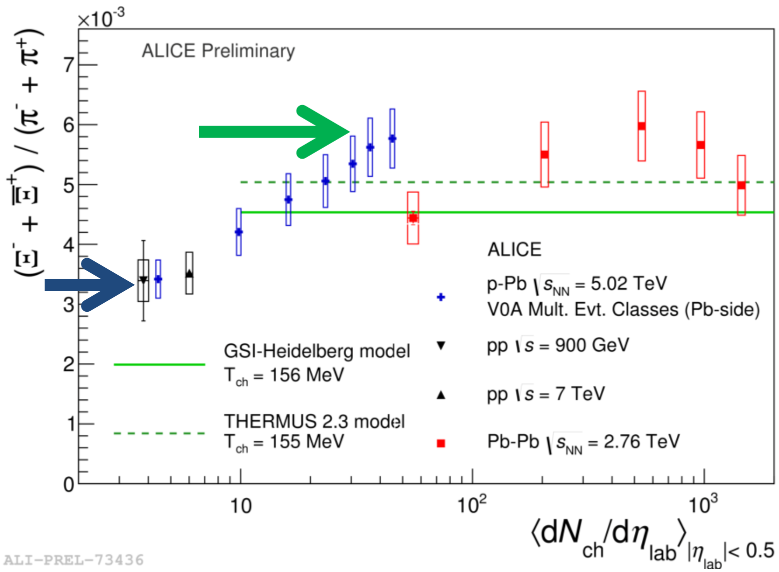

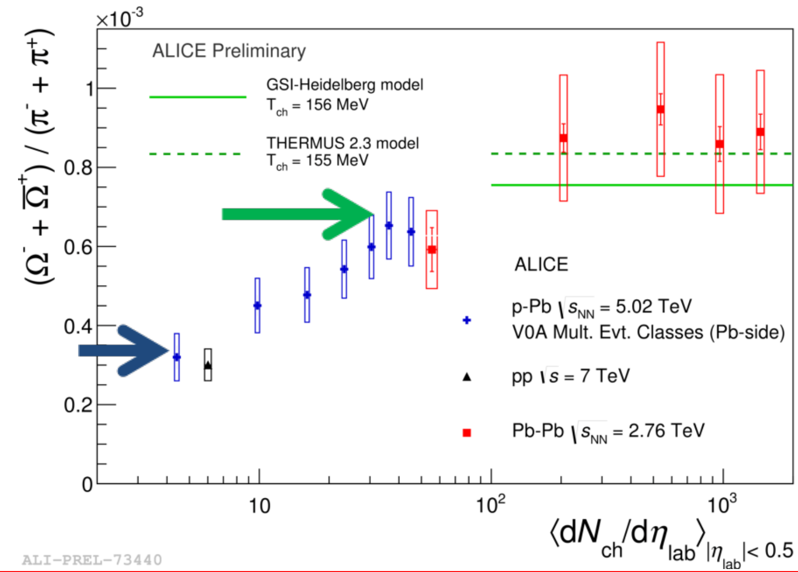

Ξ/π and Ω/π ratios in p-Pb increase with multiplicity
Low multiplicity: ratios consistent with pp
High-multiplicity: Ξ/π ~ with central Pb-Pb; Ω/π ~ with peripheral Pb-Pb

System size dependence

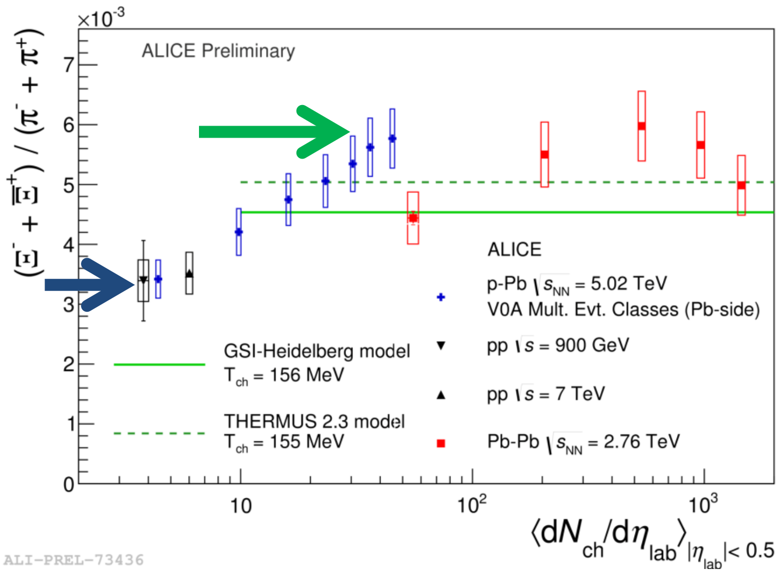

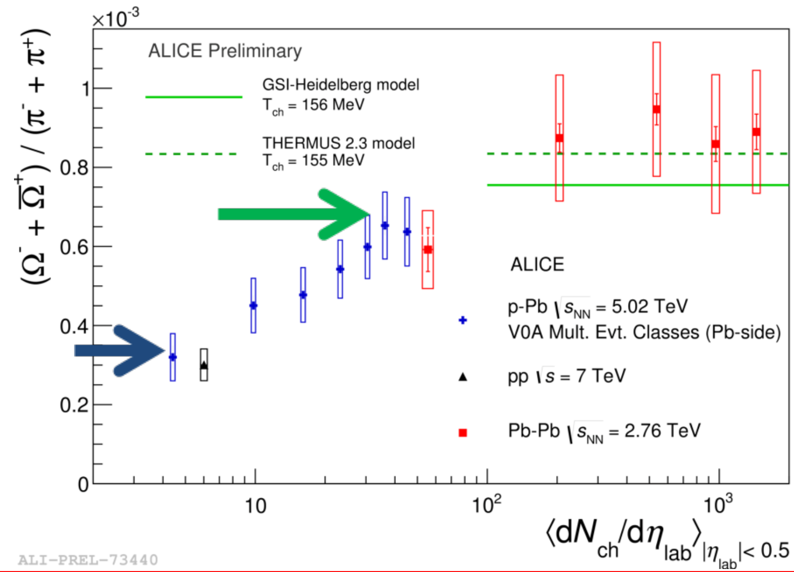

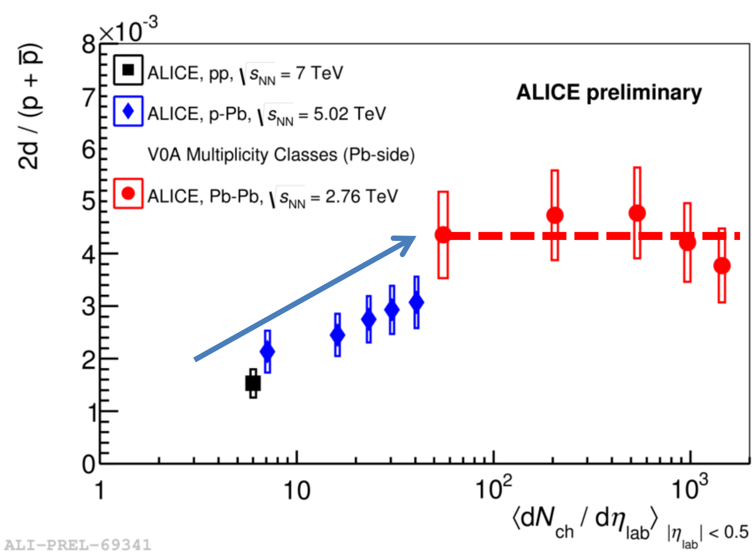

Ξ/π and Ω/π ratios in p-Pb increase with multiplicity
Low multiplicity: ratios consistent with pp
High-multiplicity: Ξ/π ~ with central Pb-Pb; Ω/π ~ with peripheral Pb-Pb

Also d/p ratio increases with multiplicity in p-Pb collisions bridging the pp and Pb-Pb values. No significant centrality dependence is observed in Pb-Pb within errors

Overview of particle production

Particle ratios evolve as a function of the system size

from small (pp), intermediate (p-Pb) to large (Pb-Pb) collision systems

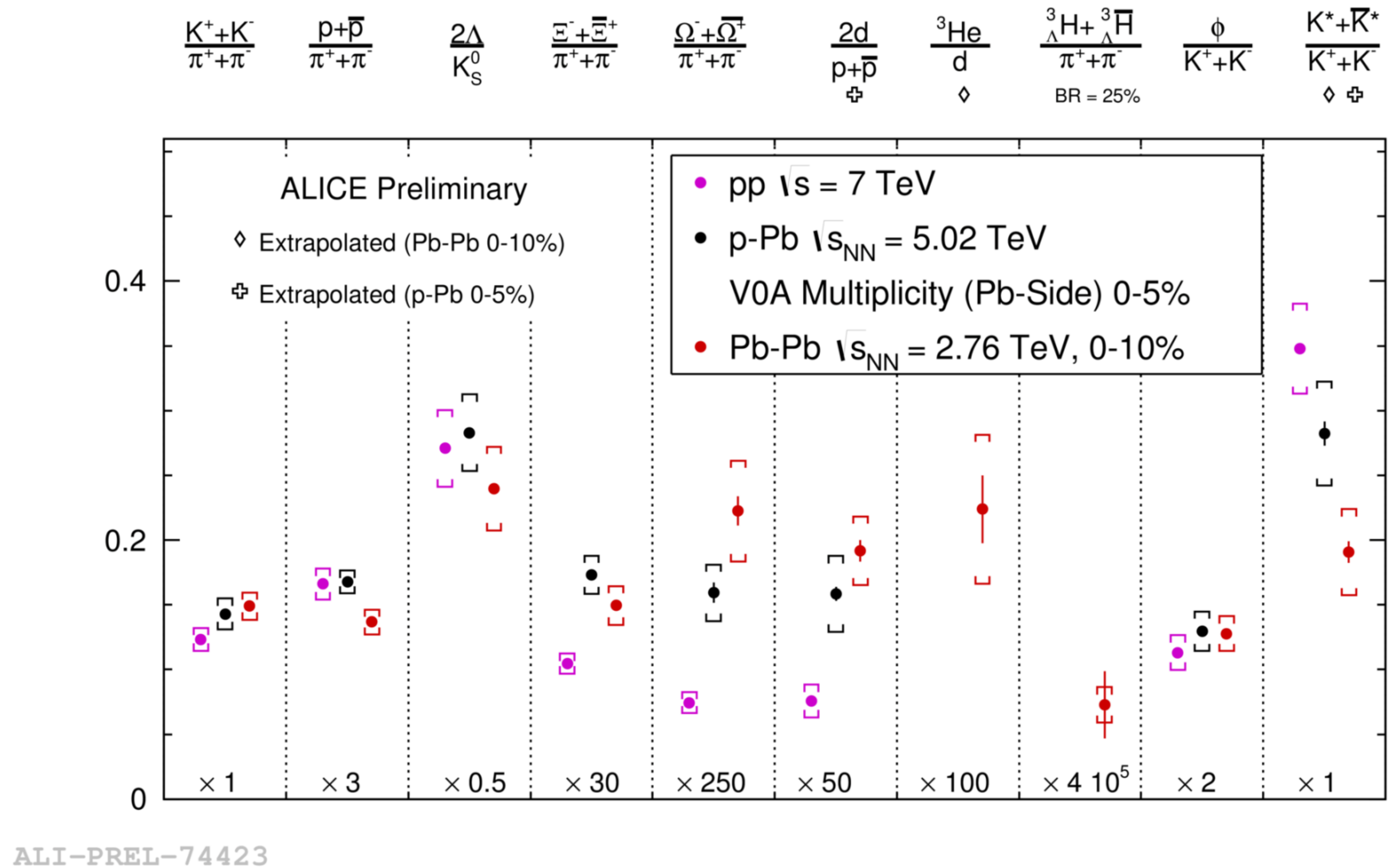

Overview of particle production

Particle ratios evolve as a function of the system size

from small (pp), intermediate (p-Pb) to large (Pb-Pb) collision systems

Strangeness enhancement

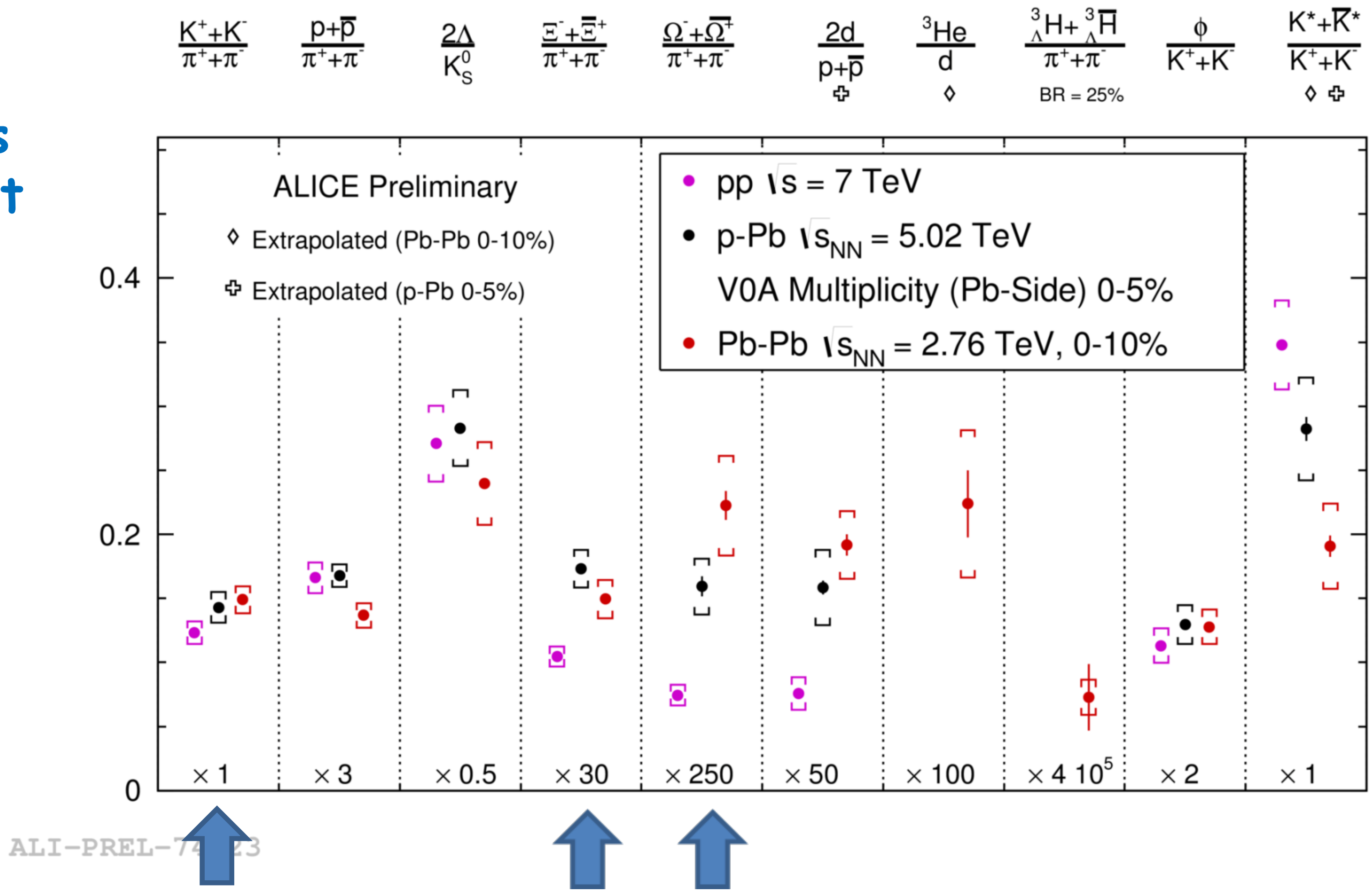

Overview of particle production

Particle ratios evolve as a function of the system size

from small (pp), intermediate (p-Pb) to large (Pb-Pb) collision systems

Strangeness enhancement

Deuteron enhancement

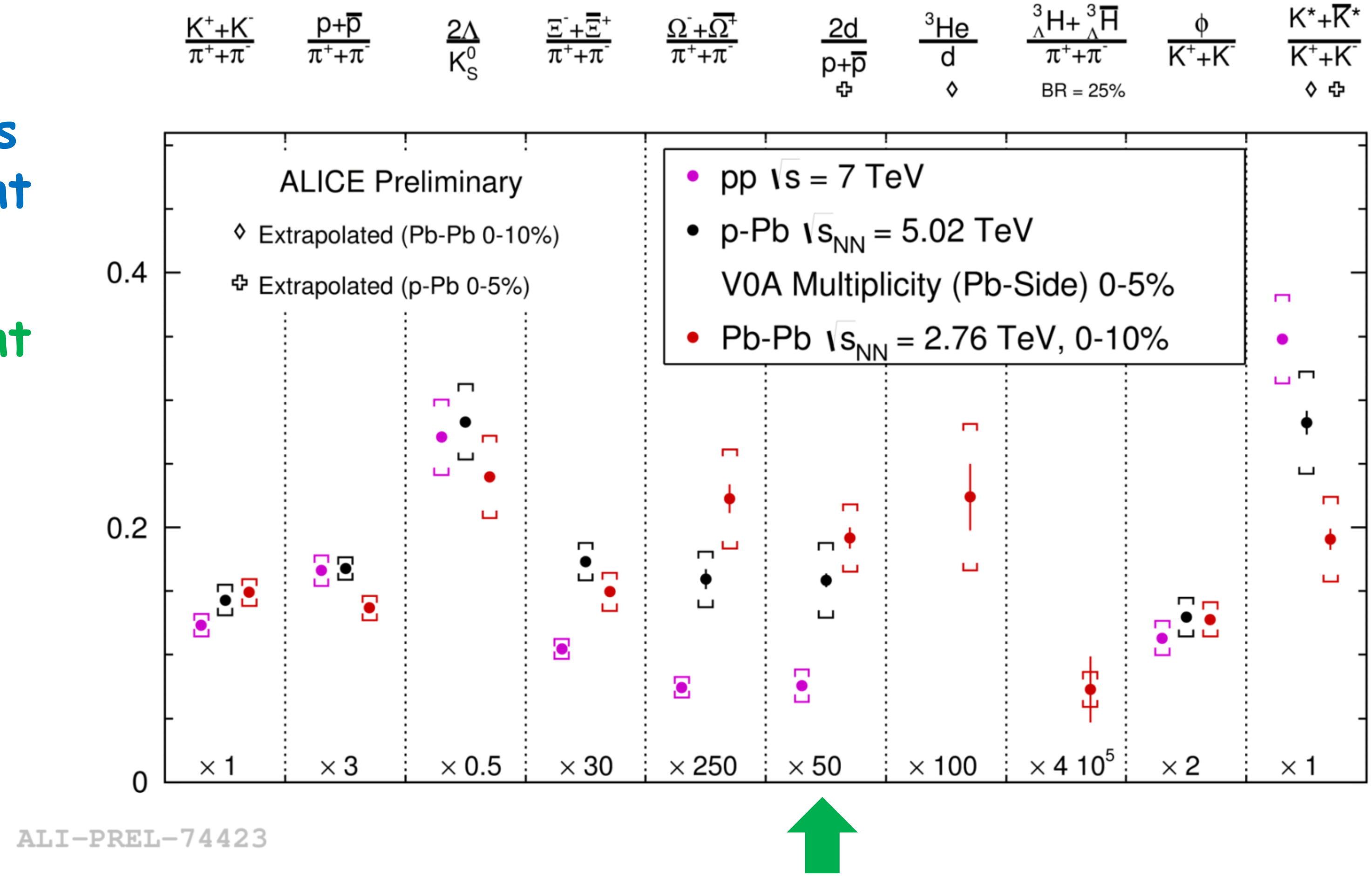

Overview of particle production

Particle ratios evolve as a function of the system size

from small (pp), intermediate (p-Pb) to large (Pb-Pb) collision systems

Strangeness enhancement

Deuteron enhancement

Baryon suppression

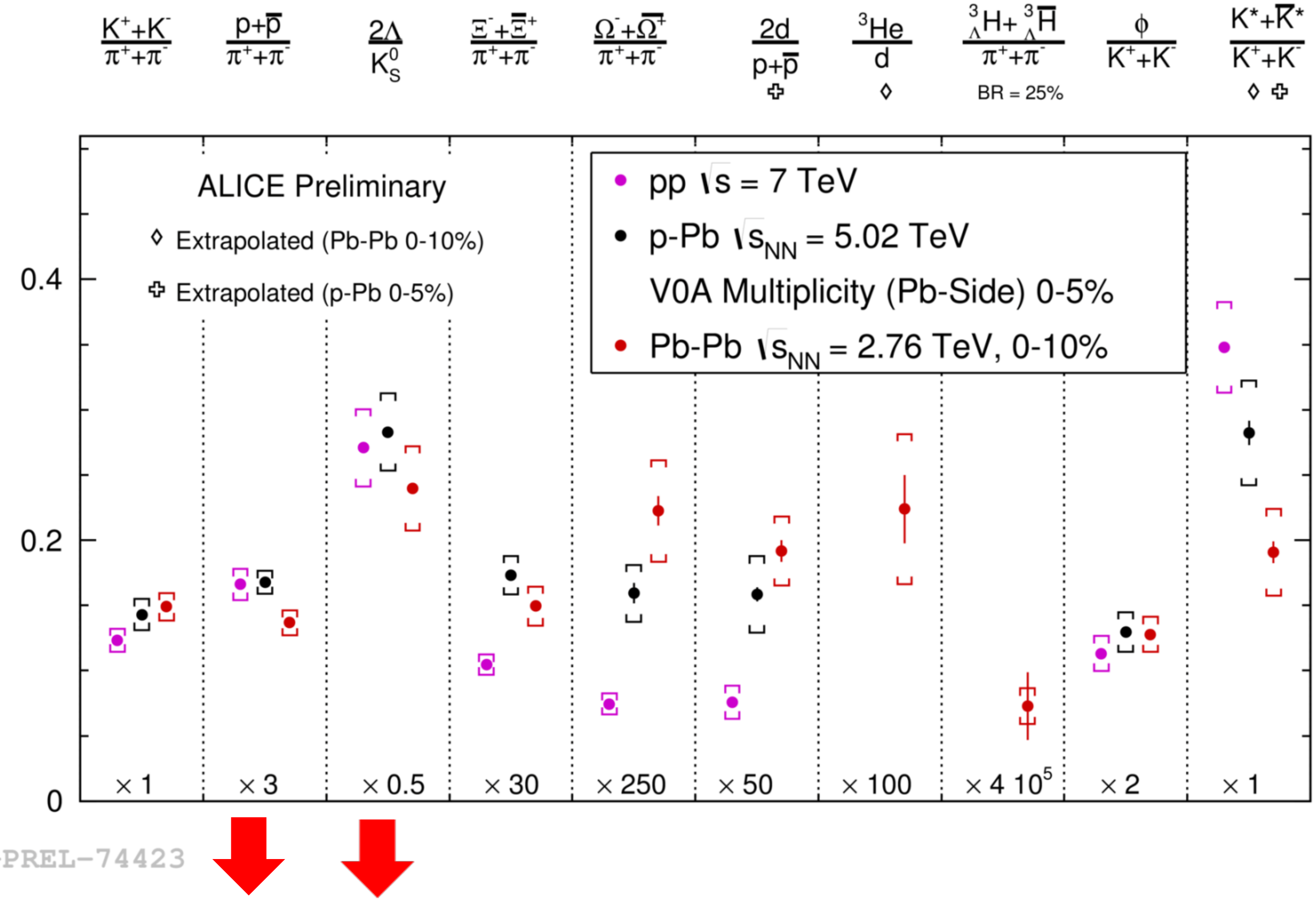

Overview of particle production

Particle ratios evolve as a function of the system size

from small (pp), intermediate (p-Pb) to large (Pb-Pb) collision systems

Strangeness enhancement

Deuteron enhancement

Baryon suppression

K* suppression

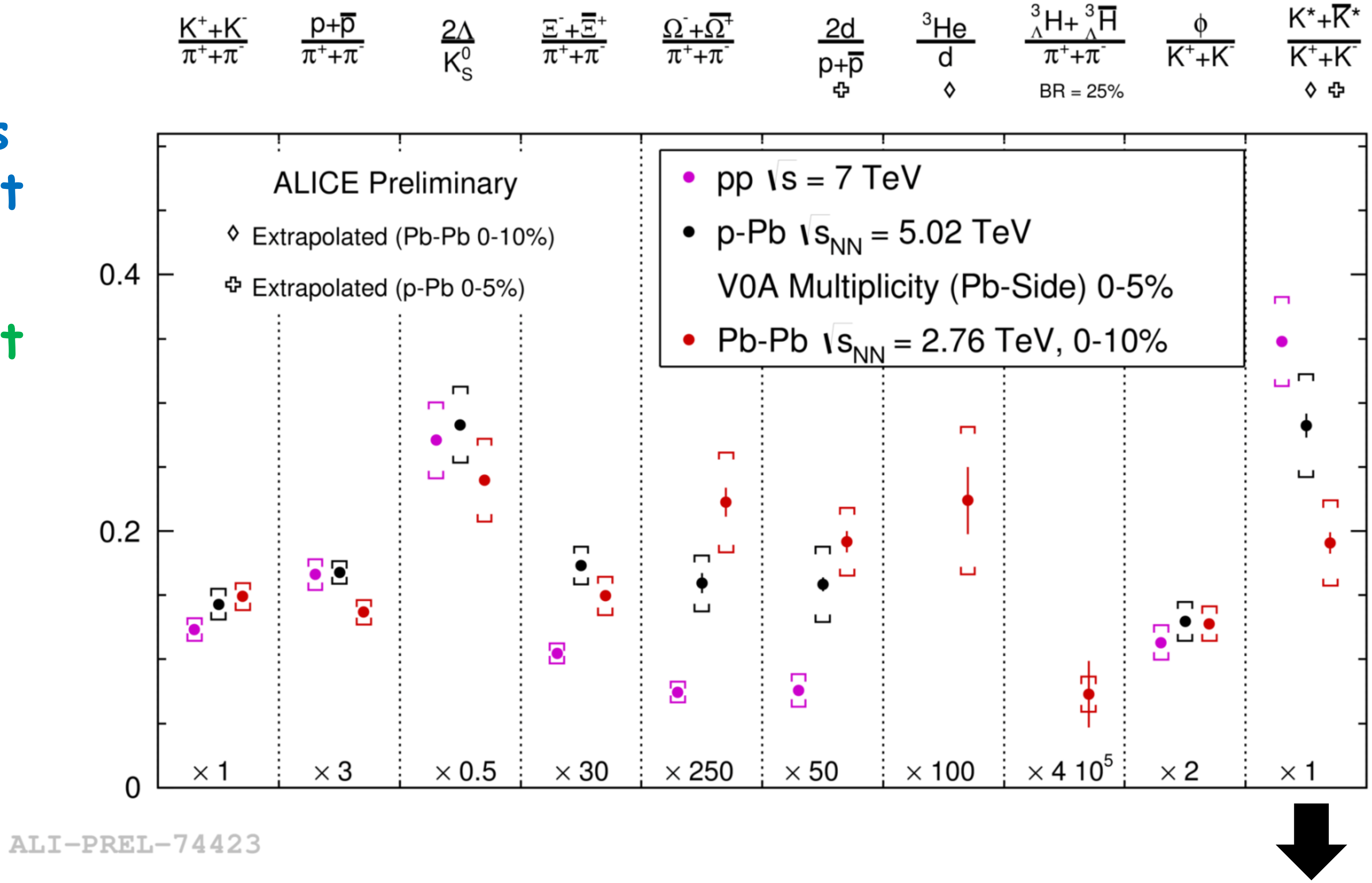

Thermal models in Pb-Pb data

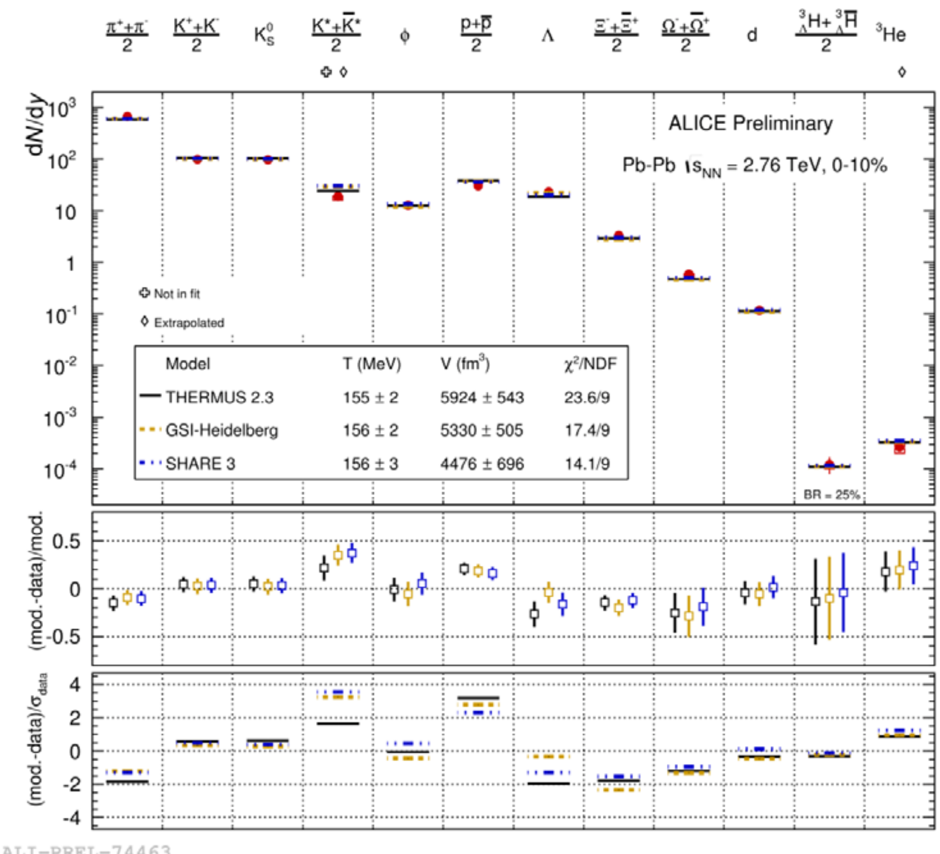

In Pb-Pb collisions at LHC energies hadrons are produced in apparent chemical equilibrium

Particle yields of light flavour hadrons (including nuclei) are described over 7 orders of magnitude with a common $T_{chemical}$=156 ± 2 MeV (prediction from RHIC extrapolation was of 164 MeV).

Three different versions of thermal model implementations give similar results

K^{*0} is not included in the fit (interaction in the hadronic phase)

Largest deviation observed for protons (incomplete hadron list, baryon annihilation in final hadronic matter,…?)

(THERMUS) Wheaton et al., Comput. Phys. Commun. 180 (2009) 84
(GSI) Andronic et al., PLB 673 (2009)142
(SHARE 3) Petran et al., arXiv 1310.5108

Thermal model in p-Pb

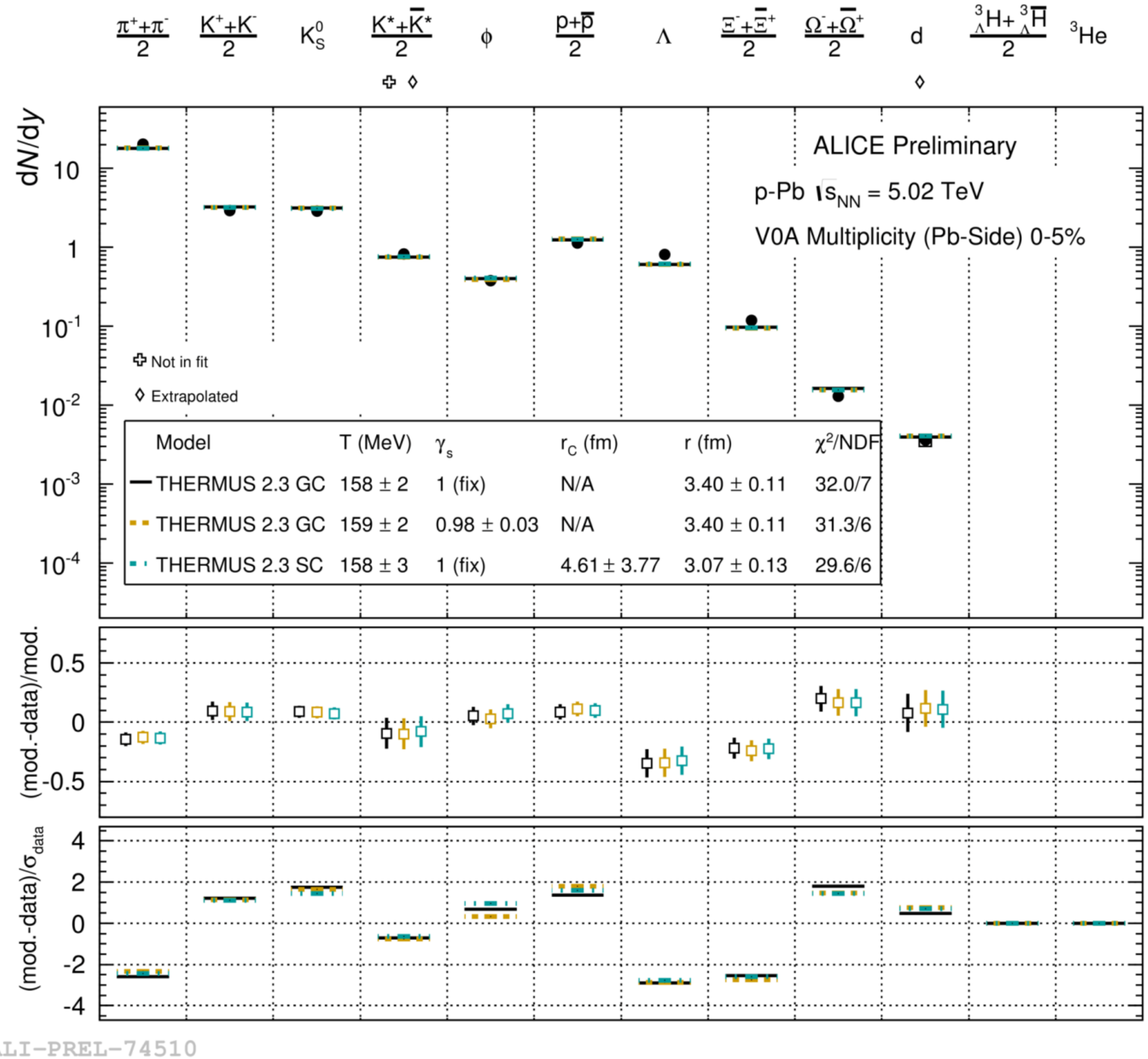

The thermal fit works to first order also in p-Pb collisions, however, the χ^2/n_{dof} is slightly worse: $\approx$5 instead of $\approx$2, mainly due to multi-strange particles

The matter created in p-Pb collisions seems to be not in chemical equilibrium, but is maybe *approaching* it

Summary

- Detailed study of the properties of the hot QCD matter shows clear signatures of a collectivity in Pb-Pb collisions

- Bulk particle production in p-Pb shows Pb-Pb features and signatures of collectivity: mass-dependence of p_T spectra and flow, but we should be aware that also non-collective effects can mimic flow-like patterns.

- Particle production changes with increasing system size: baryon and K* suppression, strangeness and deuteron enhancement

- Light flavour hadron yield can be described in a thermal fit with a chemical freeze-out temperature T_{chem} = 156 MeV. Production of light (anti-)nuclei is found to be in agreement with thermal model expectations despite their low binding energies ($T_{chem} > T_{kin} \gg E_B$).

Thanks

BACKUP SLIDES

Hypertriton lifetime

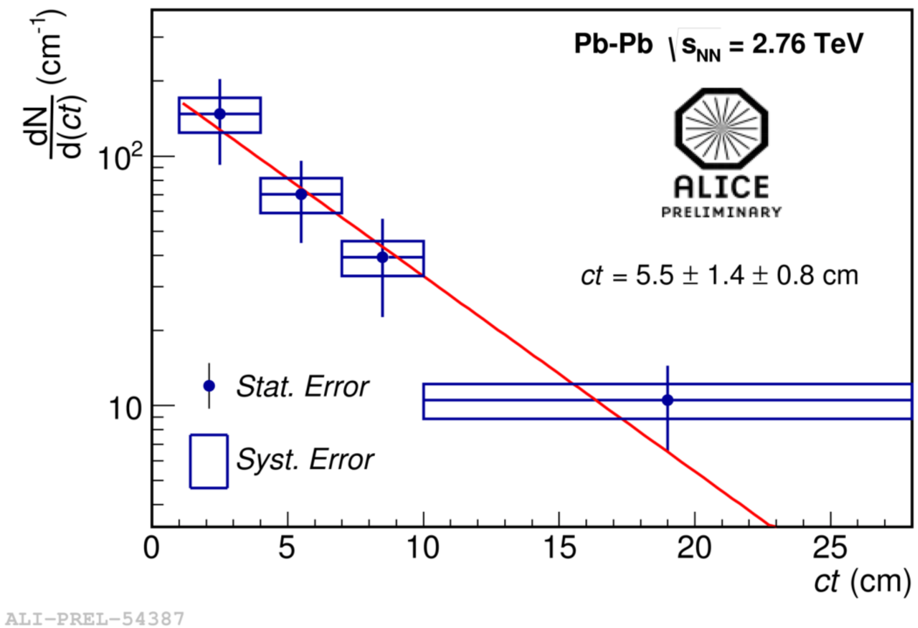

To determine the lifetime the $^{3}_{\Lambda}H$ sample has been divided in 4 intervals

$$ct = \frac{mLc}{p}$$

m = the hypertriton mass
L = decay lenght
p = total momentum

The lifetime has been determined by an exponential fit

$$N(t) = N(0)\exp\left[-\frac{t}{\tau}\right] = N(0)\exp\left(-\frac{L}{\beta\gamma c\tau}\right)$$

Coalescence parameter for deuteron

Within the coalescence model, nuclei are formed by protons and neutrons which are nearby in phase space and exhibit similar velocities. The key parameter is the coalescence parameter

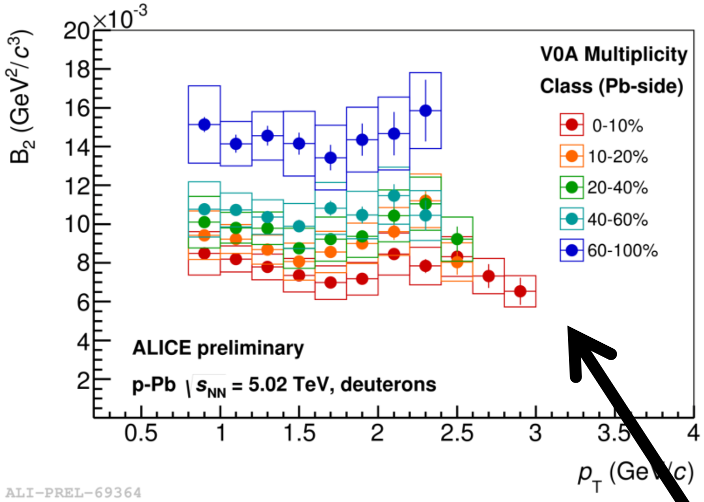

$$B_2 = \frac{E_d \frac{d^3N_d}{dp_d^3}}{\left(E_p \frac{d^3N_p}{dp_p^3}\right)^2}$$

Coalescence parameter for deuteron

At first order B_2 is expected to depend only on the maximum relative momentum of the costituent nucleons

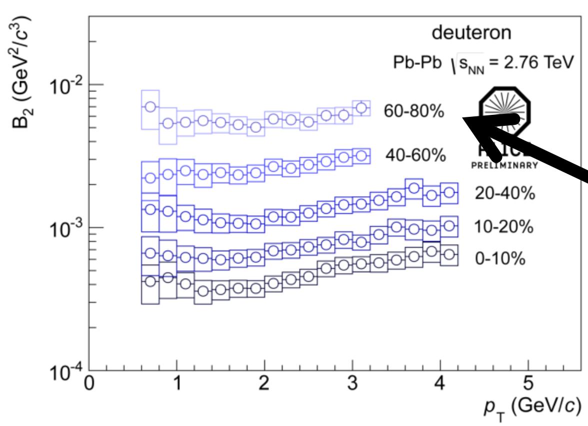

Flat B_2 vs p_T and no dependence on multiplicity/centrality → Observed in:

- p-Pb collisions
- peripheral (60-80%) Pb-Pb collisions

Coalescence parameter for deuteron

Within the coalescence model, nuclei are formed by protons and neutrons which are nearby in phase space and exhibit similar velocities. The key parameter is the coalescence parameter

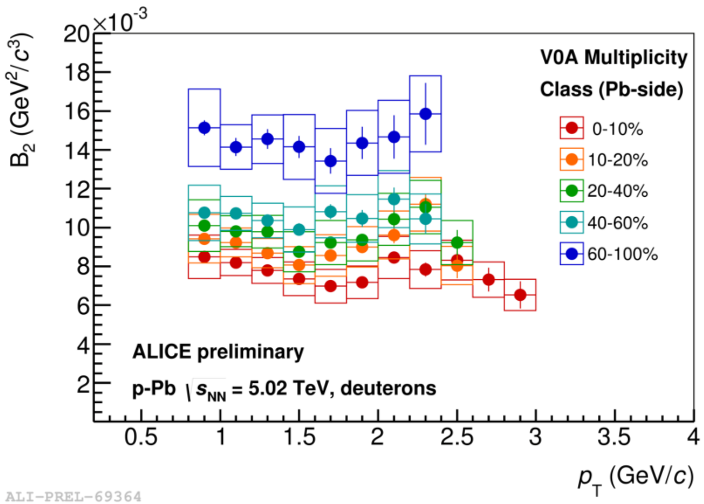

$$B_2 = \frac{E_d \frac{d^3 N_d}{dp_d^3}}{\left(E_p \frac{d^3 N_p}{dp_p^3} \right)^2}$$

Coalescence parameter for deuteron

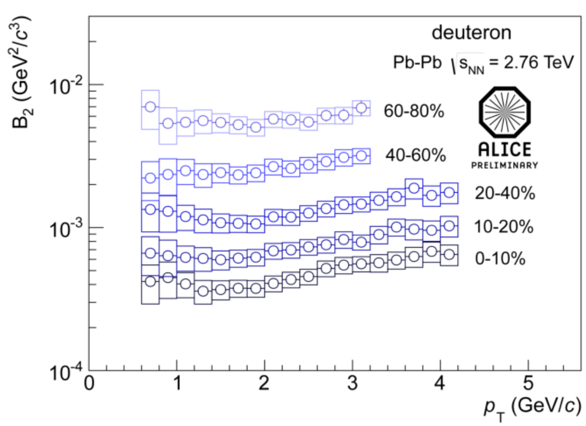

In second order, B_2 scales like HBT volume. This could explain the observed trends of B_2 in Pb-Pb collisions:

- B_2 decrease with centrality → it is due to the increase in the source volume
- B_2 increase with p_T in central collisions → reflects the k_T-dependence of the homegeneity volume in HBT

R. Scheibl and U. Heinz, PR C59(1999)1585

Coalescence Model and HBT

The size of the emitting volume has to be taken into account: the larger the distance between the protons and neutrons, lower their probability to coalesce

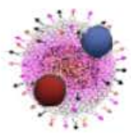

(small fireball)

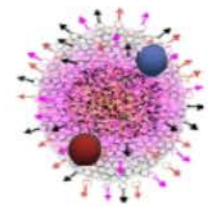

(large fireball)

$$B_2 = \frac{3\pi^{3/2}\langle C_d \rangle}{2m_T R_\perp^2(m_T) R_p(m_T)} \exp\left(2(m_T - m_0)\left(\frac{1}{T_p^*} - \frac{1}{T_d^*}\right)\right)$$

The coalescence process is governed by the same lenght of homegeneity which can be extracted from the HBR radii . $B_2 \propto 1/V_{eff}$

R. Scheibl and U. Heinz, PR C59(1999)1585

Nuclei and non-equilibrium models

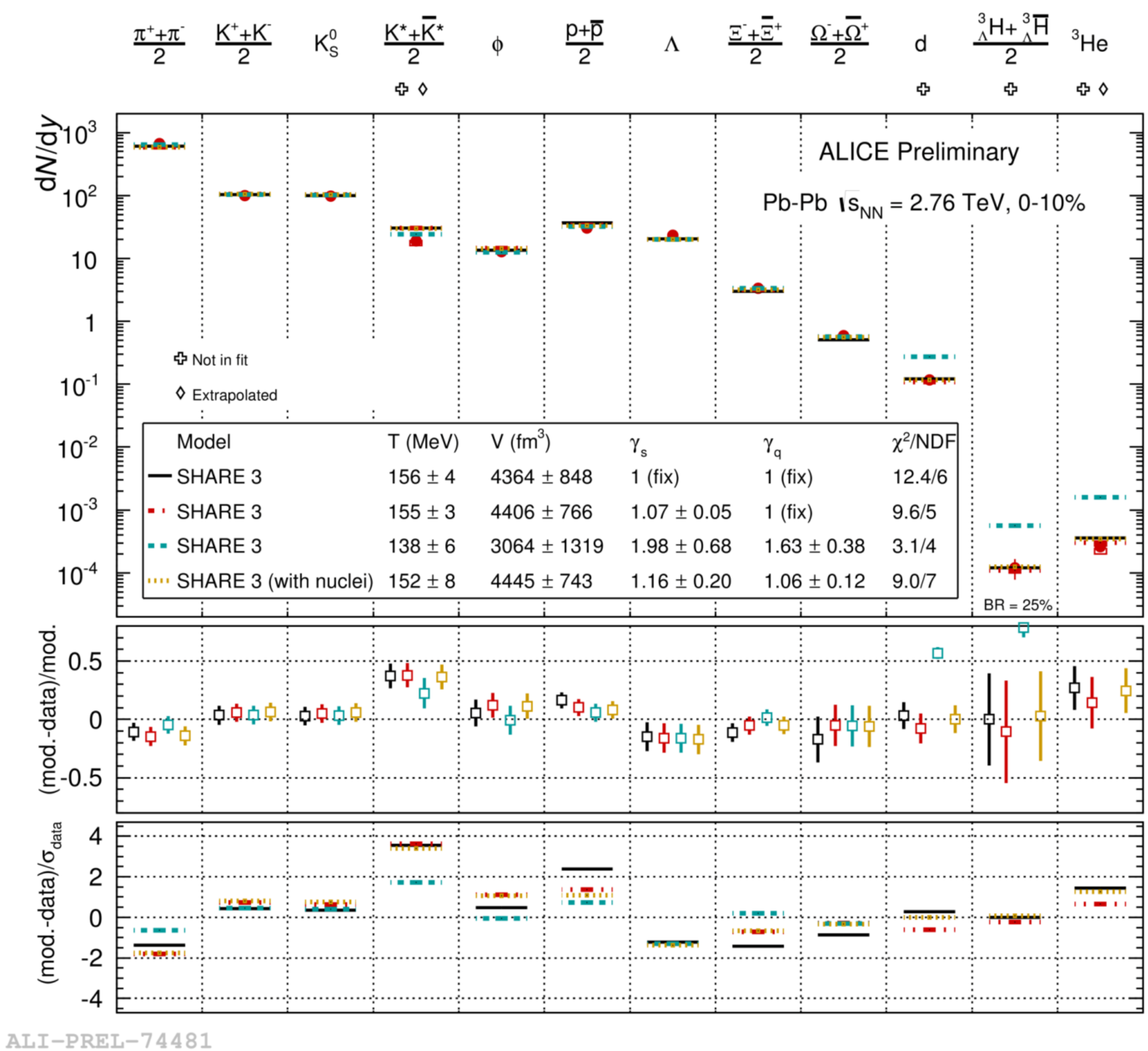

SHARE can do a thermal fit in an equilibrium mode (γ_q=γ_s=1) or in a non-equilibrium mode (γ_q and γ_s free)

In the equilibrium mode, the model describes the nuclei yields

In non-equilibrium mode and if nuclei are not included, the model converge to values of γ_q and γ_s, significantly different from 1. Hadron yields are well described , better description of protons and Ξ. Nucleus yields are largely overestimated.

In non-equilibrium mode and if nuclei are included, the model converges to values of γ_q and γ_s in agreement with 1.